

Linear and Nonlinear Buckling Analyses of Plates using the Finite Element Method

Mert Muameleci



Master thesis in Solid Mechanics performed at
Linköping University
for
Saab Aeronautics

LIU-IEI-TEK-A--14/01954--SE

Division of Solid Mechanics
Department of Management and Engineering
Linköping University, SE-581 83, Linköping, Sweden

Linköping, June 2014

**Linear and Nonlinear Buckling Analyses
of Plates using the
Finite Element Method**

**Linjära och Olinjära Bucklingsanalyser
av Plattor med hjälp av
Finita Elementmetoden**

Mert Muameleci

LIU-IEI-TEK-A--14/01954--SE

Division of Solid Mechanics
Department of Management and Engineering
Linköping University, SE-581 83, Linköping, Sweden

Linköping, June 2014

Supervisor: Bo Torstenfelt, Linköping University
Supervisor: Thomas Gustavsson, Saab Aeronautics
Examiner: Kjell Simonsson, Linköping University
Student reviewer: Michael von Rosen, Linköping University

PREFACE

The work presented in this report is my final assignment towards the degree as Master of Science in Mechanical Engineering. The work has been initiated by and carried out at Saab Aeronautics.

First, I would like to thank my supervisor Thomas Gustavsson for his endless patience, support and guidance during the course of this study. For valuable discussions and helpful inputs during my work I would like to thank all my colleagues at Saab Aeronautics, in particular Zlatan Kapidzic and Anders Bredberg. I want to thank my co-supervisor Bo Torstenfelt and my examiner Prof. Kjell Simonsson at Linköping University for their review of this report.

I'm very grateful to my family for their love and daily encouragement during these years. I could not have done it without you. Finally, I would like to thank all my friends for their support and for always helping me to perform my very best.

Linköping, June 2014

Mert Muameleci¹

¹ Email: mertmuameleci@hotmail.com or mermu243@student.liu.se

ABSTRACT

This work mainly investigates the buckling behavior of plates but also the capabilities of MSC Nastran and Abaqus for performing linear and nonlinear buckling analyses. The work starts with a literature survey on what has been investigated earlier with respect to buckling of plates. Furthermore, some plate buckling theory and how to perform a buckling analysis from a Finite Element (FE) point of view is presented.

The first part of the main work consists of a parametric study, which is performed in order to gain knowledge about how the buckling load is affected when parameters such as geometry, mesh density, type of load and boundary conditions are varied. The results from the parametric study are compared against handbook methods when possible in order to see what level of complexity is needed in the FE models to match the theory.

Furthermore, the gained knowledge from the parametric study is then used and validated in the second part where the results from FE models are compared against experimental results. The experiments are carried out on three types of HSM Shear Web Beams, one standard model (Type 5), one standard model without reinforcements (Type 1) and one standard model containing holes (Type 5).

To summarize, the main conclusions are:

- Minimum mesh density for a plate loaded in uniaxial compression and in-plane shear should be at least 4 and 8 elements per half wave, respectively, to get results within 5% error with respect to theory.
- Linear buckling analyses of simply supported plates give correct results for slender plates where buckling occurs clearly before the yield limit of the material. Nonlinear buckling analyses of plates with material nonlinearity and large displacements are fully consistent with buckling curves in the current handbook methodology.
- FE models of simply supported plates loaded in in-plane shear, containing centrally placed holes where $d/b \geq 0.225$ gives lower buckling load if compared to the handbook method. Simply supported plates loaded in in-plane shear and containing eccentrically placed holes that has a hole diameter that fulfills the condition $0.1 \leq d/b$, should be used with carefulness if placed in the compression diagonal.
- Landings of reinforced plates should be modeled in the same plane as the plate itself if shell elements are going to be used for discretizing the problem.
- Applying imperfections can reduce the buckling resistance significantly if amplitudes over 5% of thickness are used.
- The results from the FE models of the HSM Shear Web Beams show very good agreements for Type 1 and Type 5. The FE model Type 2 containing a large hole doesn't catch the right stiffness and over predicts the buckling resistance of the structure.
- MSC Nastran and Abaqus give both the same results when performing both linear and nonlinear buckling analyses.

SAMMANFATTNING

Det här arbetet undersöker huvudsakligen bucklingsbeteendet hos plattor men också möjligheterna när det kommer till att utföra linjära och olinjära bucklingsanalyser i MSC Nastran och Abaqus. Arbetet börjar med en litteraturstudie om vad som har undersökts tidigare med avseende på buckling av plattor. Därefter presenteras bucklingsteori och hur en bucklingsanalys bör genomföras från ett Finita Element (FE) perspektiv.

Första delen utav huvudarbetet består av en parameterstudie som genomförs för att få kunskap om hur bucklingslasten påverkas när parametrar som geometri, meshdensitet, last och randvillkor varierar. Erhållet resultat i parameterstudierna valideras mot nuvarande handboksmetoder då det är möjligt för att kunna kvantifiera komplexiteten som krävs i en FE modell för att återspegla teorin.

Kunskapen som erhållits i parameterstudierna används och valideras sedan i den andra delen av huvudarbetet där resultat från FE modeller jämförs med experimentella resultat. Experimenten är genomförda på tre typer utav HSM Livskjuvplåtsbalkar, en standardmodell (Typ 5), en standardmodell utan förstärkningsram (Typ 1) och en standardmodell med hål (Typ 2).

För att summera, så är de huvudsakliga slutsatserna följande:

- Minsta meshdensitet för en platta belastad i skjuv eller tryck är 4 respektive 8 element per halvvåg för att hamna inom ett fel på 5 % i förhållande till teorin.
- Linjära bucklingsanalyser av fritt upplagda plattor ger korrekta resultat för slanka plattor där buckling sker före materialets sträckgräns. Olinjära bucklingsanalyser av plattor med olinjär materialdata and stora deformationer är fullt enhetliga med bucklingskurvor i nuvarande handboksmetoder.
- FE modeller av fritt upplagda plattor belastade i skjuvning med centralt placerade hål där $d/b \geq 0.225$ ger lägre kritisk bucklingsspänning jämfört med nuvarande handboksmetoder. Fritt upplagda plattor belastade i skjuvning och med excentriskt placerade hål där diametern på hålet uppfyller $0.1 \leq d/b$ bör användas med försiktighet om hålet placeras längs tryckdiagonalen.
- Förstyvningar hos plattor bör modelleras i samma plan som plattan själv om skalelement skall används för att diskretisera problemet.
- Imperfektioner med amplitud över 5 % av tjockleken bör användas med försiktighet, då en detaljs bucklingsmotstånd kan sjunka avsevärt.
- Resultaten från FE modellerna av HSM Livskjuvplåtsbalkarna visar väldigt god överensstämmelse för Typ 1 och Typ 5. FE modellen av Typ 2 med ett stort hål lyckas inte beskriva detaljens styvhet korrekt och förutspår en alltför hög bucklingslast.
- Både MSC Nastran och Abaqus ger båda samma resultat för linjära och olinjära bucklingsanalyser.

CONTENTS

PREFACE.....	iii
ABSTRACT.....	iv
SAMMANFATTNING.....	v
CONTENTS	vi
CHAPTER 1 INTRODUCTION.....	8
1.1 Information about Saab	8
1.2 Background	9
1.3 The objective	11
1.4 Limitations and simplifications	12
1.5 Additional considerations	13
CHAPTER 2 APPROACH.....	14
2.1 General	14
2.2 Literature survey	15
2.3 Part 1	16
2.3.1 Part 1.1.....	16
2.3.2 Part 1.2.....	16
2.3.3 Part 1.3.....	17
2.3.4 Part 1.4.....	17
2.3.5 Part 1.5.....	18
2.3.6 Part 1.6.....	18
2.3.7 Part 1.7.....	18
2.3.8 Part 1.8.....	18
2.4 Part 2	19
CHAPTER 3 THEORY.....	20
3.1 The Finite Element Method (FEM)	20
3.2 Plate Buckling Theory	22
3.3 Buckling and Finite Element approach	24
3.3.1 Fundamentals of Buckling Analysis using FEM	24
3.3.2 Estimation of Buckling load in Nonlinear Analysis.....	28
3.3.3 Estimation of Error	29
CHAPTER 4 LITTERATURE SURVEY.....	30
CHAPTER 5 FE Modeling.....	33
5.1 General	33
5.1.1 Solver	33
5.1.2 Pre- and post processors	33
5.1.3 Boundary conditions and Load types	34
5.1.4 Material Data	35
5.2 Part 1	36
5.3 Part 2	37
5.3.1 Geometry	39
5.3.2 Material data.....	39
5.3.3 Boundary conditions.....	39
5.3.4 Element type and Mesh.....	40
5.3.5 Handbook approach	40

5.3.6 Experimental testing	41
CHAPTER 6 RESULTS & EVALUATION.....	42
6.1 Part 1.....	42
6.1.1 Part 1.1.....	44
6.1.2 Part 1.2.....	46
6.1.3 Part 1.3.....	47
6.1.4 Part 1.4.....	48
6.1.5 Part 1.5.....	49
6.1.6 Part 1.6.....	51
6.1.7 Part 1.7 and Part 1.8.....	52
6.2 Part 2.....	53
6.2.1 HSM Shear Web Beam Type 1	54
6.2.2 HSM Shear Web Beam Type 5	55
6.2.3 HSM Shear Web Beam Type 2	55
6.2.4 Summary	55
CHAPTER 7 CONCLUSIONS & FURTHER WORK	58
7.1 Conclusions.....	58
7.1 Further work.....	59
BIBLIOGRAPHY	60
APPENDIX.....	62
Appendix A: FE model setup	62
5.2.1 Part 1.1.....	62
5.2.2 Part 1.2.....	62
5.2.3 Part 1.3.....	63
5.2.4 Part 1.4.....	63
5.2.5 Part 1.5.....	64
5.2.6 Part 1.6.....	64
5.2.7 Part 1.7.....	65
5.2.8 Part 1.8.....	65
Appendix B: HSM Shear Web Beam Drawings	66
Appendix C: Pictures from Experiments on HSM Shear Web Beam	67
Appendix D: Graphs	68
Part 1.1	68
Part 1.2	70
Appendix E: Contour Plots	71
Part 2.....	71

CHAPTER 1

INTRODUCTION

This chapter contains some short information about Saab, which is the company at which this thesis work is performed, and also the background, objective and limitations of the thesis.

1.1 Information about Saab

Saab was founded in 1937 and stands for Svenska Aeroplan Aktiebolaget. Today, the main focus is in three strategic areas: Defence- and Security Solutions, Systems & Products and Aeronautical Engineering.

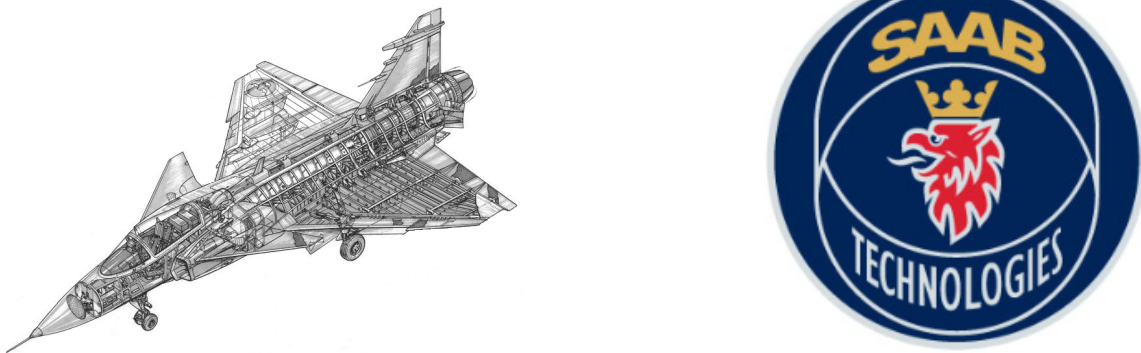


Figure 1: The logo of Saab AB (right) and a fighter aircraft (left).

There are currently about 14 000 employees' at Saab and the company is divided into six business areas: Aeronautics, Dynamics, Electronic Defence Systems, Security and Defence Solutions, Support and Services and Combitech.

When it comes to aircraft production, the main focus is on fighter aircrafts. Saab has been developing and producing aircrafts since the 1930s and has creates planes like Tunnan, Lansen, Draken, Viggen and JAS 39 Gripen. The third-generation Gripen planes are now being developed (Saabgroup, 2014).

1.2 Background

Engineering of today is very challenging. A structural engineer has to ensure the integrity of the constructed structure, but also take economical, environmental and aesthetic aspects into account. Buckling is a big problem, particularly in thin-walled structures where the membrane stiffness is much greater than the bending stiffness. By definition, a thin-walled structure is a three-dimensional component where one dimension is very small in comparison to the other two and typical examples are plates, thin-walled cylinders, arches and shells.

The desire of low-weight, high strength and high fuel efficiency in the aviation industry has led to that structures of this type, because of its properties, are very applicable within this particular area of engineering. Unfortunately, these structures possess the property of being very sensitive to geometrical and mechanical imperfections. This, in combination with the restricted bending stiffness, makes buckling one of the most important failure criteria in these type of structures.

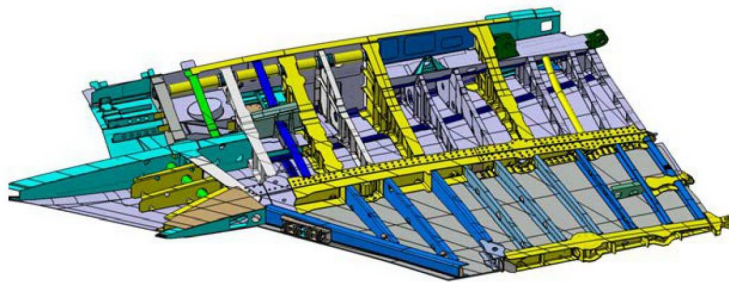


Figure 2: Wing Structure of the JAS39 Gripen aircraft.

Buckling in engineering structures is highly sensitive to imperfections; these imperfections can be of varying types e.g. different directions of fiber design, thickness variations, perforations or residual stresses. The loading conditions are also an important parameter that affects the buckling behavior of a structure. A structural part in service can be exposed to any variation of loads in a large number of cycles.

During the normal service life of an airplane structure, e.g. a stiffened panel, it may be exposed to thousands of buckling cycles, which is also an argument for why it is important to develop appropriate methodologies to predict and handle the behavior with respect to buckling.

The buckling phenomena can be divided into two parts: global buckling and local buckling. Typical example of global buckling is when the whole structure buckle as one unit, while examples of local buckling is when the skin buckles in a stiffened panel or some minor buckling around an unstiffened hole, see Figure 3.

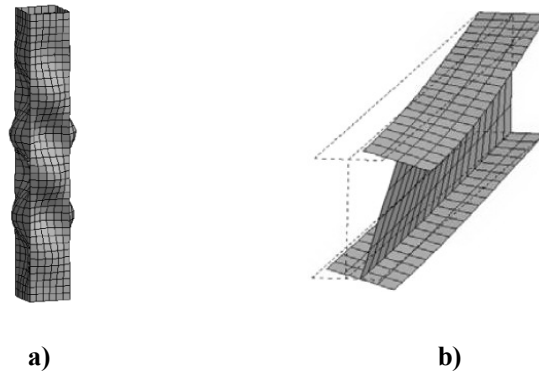


Figure 3: Two types of buckling; a) Local buckling and b) Global buckling.

The use of Finite Element (FE) analyses for investigating the buckling resistance of structures has increased a lot during the last decade and this is mainly because of the improvements in computational capacity. The typical way of making a FE structural analysis of an aircraft is illustrated in Figure 4.

The analysis starts from a global structural model based on sub-structuring technique to make analyses with respect to many load cases. Furthermore, a load distribution analysis is performed on a smaller structural part. Finally, after the load distribution analysis, a smaller local stress or buckling analysis is performed where the input comes from the results obtained in the previous step (Korolija, 2012).

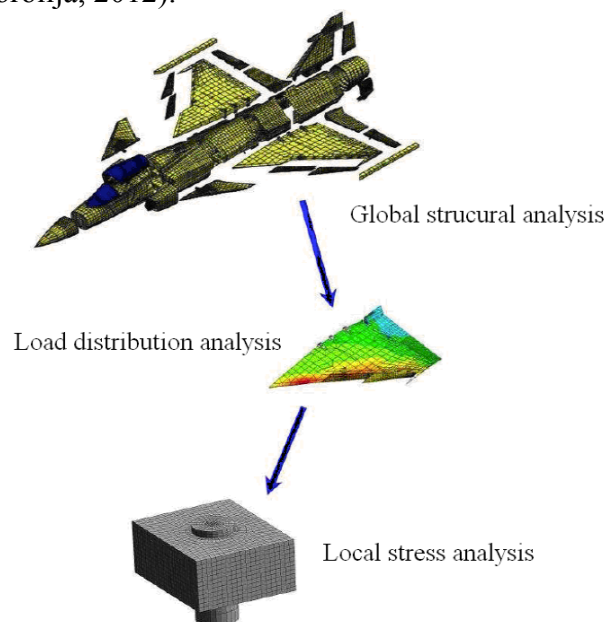


Figure 4: Different steps when making a FE structural analysis of an aircraft.

The amount of complexity included in a local stress or buckling analysis can differ but it is possible to include a large amount of different phenomena at the expense of computational time.

1.3 The objective

The main objective of this thesis is to improve the current knowledge about linear and nonlinear buckling analyses using the Finite Element Method (FEM), i.e. to give recommendations for modeling problems where this phenomenon has to be considered. It is also of interest to compare and validate the results obtained from the Finite Element (FE) analyses against the Strength Data handbook of Saab, in order to find limitations in current methodology if compared against numerical methods.

The handbook methods are used for calculating the critical buckling load of plates with various geometries, boundary conditions and exposed to loading types such as in-plane shear and/or uniaxial compression.

At Saab, all linear FE analysis is performed using MSC Nastran as a solver while Abaqus is utilized for nonlinear analyses. These are two different solvers that have different capabilities within different areas of computational engineering and it is of interest for Saab to compare these two solvers against each other with respect to precision, speed, and simplicity.

Today, when performing nonlinear analysis, models are often converted from MSC Nastran to Abaqus and this conversion may not always be 100 percent perfect. This incompatibility leads to that extra work that has to be done by the engineer before the analysis can be run with the Abaqus solver. To skip this extra step and to be able to perform both local and global FE analyses directly using the same solver, validating the nonlinear solving capabilities of MSC Nastran is of interest.

1.4 Limitations and simplifications

Following limitations were imposed during the work:

- The plates are assumed to be perfectly flat and loaded in in-plane shear or uniaxial compression and the boundary conditions are either simply supported or clamped (even though most of the cases are simply supported). As choice of element, shell elements are used in the Finite Element models.
- In nonlinear buckling analysis, the method for evaluating if a structure buckles or not is always evaluated by using a force (or Load Proportionality Factor) versus the out-of-plane displacement.
- MSC Nastran and Abaqus have both their own four-node shell element formulation implemented. When converting models from MSC Nastran to Abaqus, the pre-processor converts a CQUAD4 element from MSC Nastran to an S4 element in Abaqus. These are two four-node shell elements that have mathematical differences in their formulations, but these differences are not investigated further in this study and they are assumed to be equivalent as elements.
- The QUAD4 element is used in the simulations, even though the QUAD8 element would show much faster convergence for flat plates. One of the reasons is that Saab uses the QUAD4 element in their global FE models in MSC Nastran with the motivation that MSC Nastran has the K6ROT and SNORM parameters that makes it possible to handle the rotation stiffness in the element normal direction in a good way. These features are not available when using the QUAD8 element. The second reason is that MSC Software itself does not recommend using their QUAD8 element.
- The first eigenmode is always imposed as the choice of imperfection when performing nonlinear buckling analysis, with the motivation that the structure will most likely buckle in this mode. No studies have been done on how the buckling load will be affected if a sum of the first eigenmodes are scaled and used as imperfections. In reality, analyses would need to be carried out to ensure that the use of the first eigenmode gives conservative and safe results.
- The results from the experimental testing of the High Speed Machining (HSM) Shear Web Beam type 2 and type 1 is just considered with respect to the load level at which buckling occurs. The whole buckling path is not used in the comparison because of lack of data. Also, the buckling paths are just evaluated with respect to where the buckling occurs (up to 30% of applied load) and not for further loading where plasticity also takes place.

1.5 Additional considerations

The conducted work has no obvious potentially negative environmental impacts. Furthermore, no gender related issues are raised by the work.

Finally with respect to ethical and moral aspects, Saab develops defense material that is aimed at increasing the safety of the citizen and which is done in accordance with the Swedish law system.

CHAPTER 2

APPROACH

This chapter contains the approach for how the work is going to be performed, description of the different parts in the thesis and furthermore gives an overall view of the work scheme.

2.1 General

In order to improve the knowledge about how the buckling load of plates is affected when geometrical parameters, different types of load, boundary conditions and geometrical cases are changed, a parametric study is carried out. All the parts, load cases and geometrical variations are established after discussions with the supervisor and therefore also with respect to the current area of interest at Saab. The approach for satisfying the main objective is divided into two main parts and a literature survey.

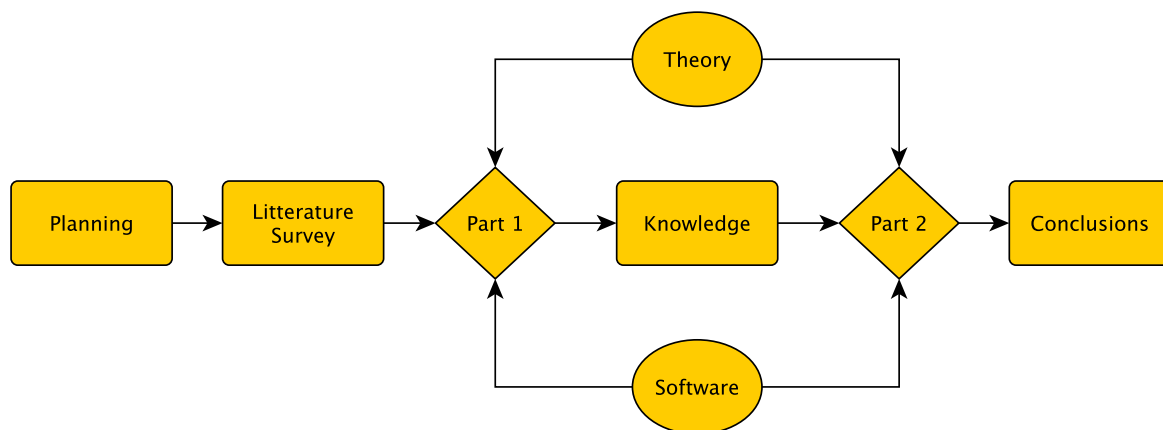


Figure 5: Schematic view over the work procedure for the thesis.

In studies of a numerical character, such as this, it is essential to deploy a satisfactory foundation of previous research within the field of buckling – hence the need of an adequate literature survey. The synthesis of the survey's outcome will then form the theoretical background to the first part of the thesis.

The aim of the first part is to perform parametric studies where the impact on the buckling load of variables such as geometry, boundary conditions and load cases are studied. The idea is, based on the collected data from the parametric studies, learn about the limitations and requirements when it comes to performing buckling analyses for various cases, both linear and nonlinear. See Figure 6 for a schematic view of the first part of the work. Major parts of the analyses are performed in two different solvers: MSC Nastran and Abaqus. Hence, the goal is also to learn and see the capabilities within each solver.

The second part of the thesis is to, based on what has been learned in the first part, make an FE model of a test specimen and perform buckling analysis at the needed level of complexity. It is of interest to validate the predictive capabilities of the FE solver against the experiments that have been conducted. A schematic view of the second part can be seen in Figure 10 and the entire approach in Figure 5.

2.2 Literature survey

Because of the enormous amount of literature and articles available with respect to buckling analysis, some cases that were considered relevant with respect to the work performed in this thesis were selected and used as a base for the research.

Following topics were chosen to put focus on:

- *Buckling of flat plates subjected to in-plane shear and/or uniaxial compression, under clamped or simply supported conditions.*
- *Buckling of flat plates containing circular or rectangular holes with/without reinforcement.*
- *The use of geometrical imperfections on perfectly flat plates.*
- *The imperfection sensitivity of flat plates.*
- *Guidelines for mesh densities.*
- *Postbuckling behavior of flat plates and the impact of different parameters, e.g. boundary conditions and type of loading, on the postbuckling paths.*

2.3 Part 1

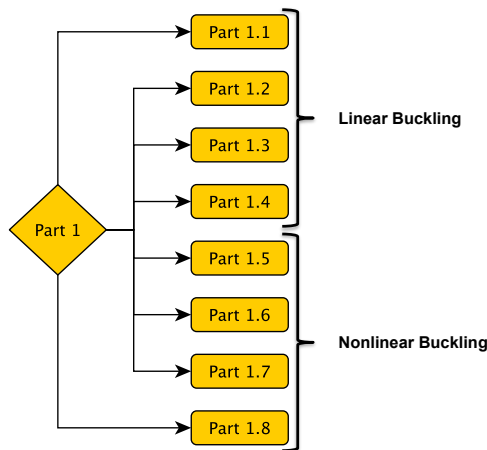


Figure 6: Schematic view of Part 1.

2.3.1 Part 1.1

The first subpart was to make a mesh convergence study. The plates considered are square or rectangular (where the longer side is four times the shorter side), simply supported or clamped, loaded in in-plane shear or uniaxial compression. Solutions are obtained with respect to different mesh densities/ratios and geometries, see Figure 7.

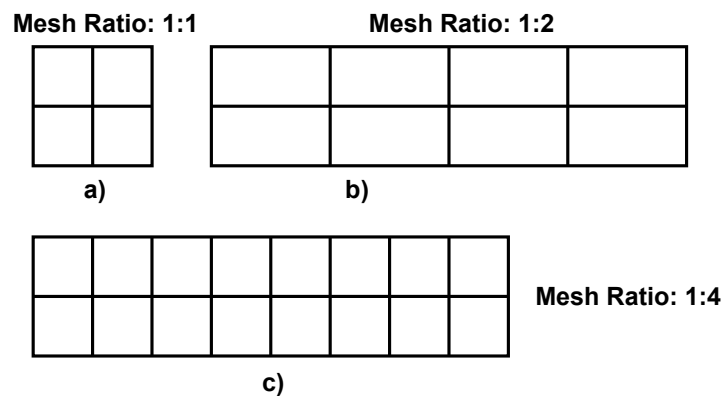


Figure 7: Different mesh ratios that were utilized in the mesh convergence study.

The analyses are mainly carried out in MSC Nastran, but a mesh convergence check using a high mesh density is also done for Abaqus. The outcome of this study is to give guidelines for the needed mesh density with respect to the different load cases and boundary conditions when performing linear buckling analysis.

2.3.2 Part 1.2

The second subpart is about evaluating current handbook methods with respect to the critical buckling load against results obtained by performing linear buckling analyses. The buckling loads from the plates that are square, simply supported and loaded in in-plane shear or uniaxial compression are validated against the buckling curves in the Strength Data handbook of Saab (SD 14-110 and SD 14-115). This is done using both MSC Nastran and Abaqus.

The aim is to investigate for which part of the buckling curves the linear buckling analysis is valid, because as the thickness increases, the buckling will occur closer to the yield limit of the material where nonlinear effects due to softening start to appear.

2.3.3 Part 1.3

The third subpart consists of evaluating the critical buckling load obtained by performing linear buckling analyses of plates containing unreinforced holes. The type of load used in these analyses is in-plane shear load and the plates are simply supported along all four edges.

Three types of placements are tested where the hole is placed in the center, translated to the right or to the corner, see Figure 8. For the case where the hole is placed to the right, the eccentricity, e , is $0.25b$ in x -direction (where b is the length of the side and the eccentricity is measured from the midpoint of the plate to the center of the hole) and for the case when the hole is placed in the corner; the eccentricity is $0.25b$ in both x - and y -direction.

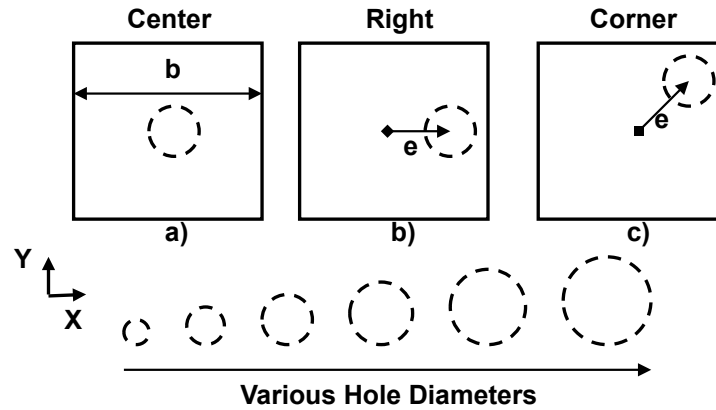


Figure 8: Various placements that have been studied in this subsection.

The aim of this subpart is to improve the knowledge about how the buckling load is affected when parameters such as diameter and placement are changed. Also, different kinds of mesh densities around the hole are used in order to explore if the obtained results are mesh-dependent.

Numerical results are validated against the Saab Strength Data handbook (SD 14-365) for the case when the hole is placed at the center, which is considered as the extreme case i.e. the case where the lowest buckling load is obtained. Most of all theory available for plates containing holes is based on the assumption that the hole is placed at the center of the plate.

2.3.4 Part 1.4

The fourth subpart is to perform linear buckling analysis and investigate how the critical buckling load for simply supported, reinforced plates, subjected to in-plane shear are affected when the landings are generated directly from CAD models for meshing with shell elements, i.e. extracted from the original geometry as midsurfaces, see Figure 9.

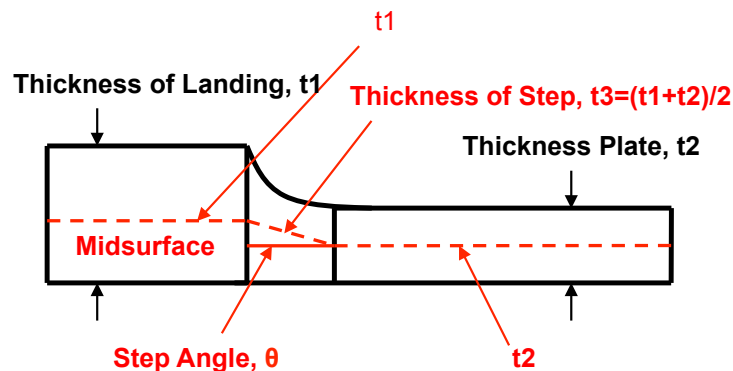


Figure 9: The midsurface extraction.

A comparison is made between this way of modeling a plate against a conventionally modeled plate, i.e. a plate where all nodes are in the same plane and the landings are represented as a change of thickness for the corresponding elements, both for shell and solid elements.

2.3.5 Part 1.5

The fifth subpart is about performing nonlinear buckling analyses containing geometrical nonlinearities. This is done in both MSC Nastran and Abaqus, for simply supported plates and for two load cases; in-plane shear and uniaxial compression.

Introducing imperfections is essential for performing nonlinear buckling analysis of perfectly flat plates, which makes one of the aims to investigate the imperfection sensitivity of plates that are exposed to the two types of load. It is also of interest to evaluate the nonlinear analysis capabilities of the two solvers that are used in this work.

Finally, two methods for approximation of the critical buckling load in nonlinear buckling analyses; the Linearization method and Second derivative method, are evaluated and compared against each other. The aim is to find the most appropriate one for use in further investigations.

2.3.6 Part 1.6

The sixth subpart is about performing nonlinear buckling analyses using both geometrical nonlinearities and nonlinear material data and investigate how well it is possible to fit the buckling curves available for different materials in the Strength Data handbook of Saab (SD 14-110 and SD 14-115).

It is of extra interest to explore how well FE models can predict the critical buckling load when it is in the area of the curves where the material shows nonlinear behavior i.e. where the plate is thick and buckles closer to the yield limit.

The used solvers for these analyses are both MSC Nastran and Abaqus.

2.3.7 Part 1.7

Part 1.3 is reconsidered but this time the buckling load is calculated by taking into account both geometrical nonlinearities and nonlinear material data.

2.3.8 Part 1.8

Part 1.4 is reconsidered but this time the buckling load is calculated by taking into account both geometrical nonlinearities and nonlinear material data.

2.4 Part 2

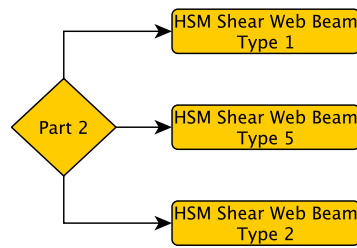


Figure 10: Schematic view of Part 2.

The aim of this part is to study the buckling behavior of the Shear Web Beam of aircraft frames and spars, manufactured with the High Speed Machining technique (HSM). A comparison is made between the results obtained from the Finite Element analyses against the experiments.

Parts that are manufactured with the HSM technique are integral structures, i.e. they are manufactured in one piece. With this way of manufacturing, the use of fasteners is minimized.

Three types of Shear Web Beams are analyzed: two standard models, with and without holes (HSM Shear Web Beam Type 2 and HSM Shear Web Beam Type 5), where the only difference between these two is the presence of holes in Type 2. The third and final model is the same as Type 5 but without any reinforcements and is named HSM Shear Web Beam Type 1. See Figure 50 – Figure 53 in Appendix B for further details regarding the geometry of the various test specimens.

CHAPTER 3

THEORY

This is a theoretical chapter containing the underlying theory for this thesis. First, it describes the very basics of the Finite Element (FE) method and then continues with Plate Buckling Theory. Furthermore, it contains a discussion about how to perform Buckling Analysis from an FE point of view and finally some theory on estimation of Buckling Load and Error.

3.1 The Finite Element Method (FEM)

The Finite Element Method (FEM) is used in a large variety of different engineering areas and is the most important tool in the field of Computer-Aided Engineering (CAE). According to Torstenfelt (2007), the method has been described in several different ways but in beginning, it was described as a Rayleigh-Ritz method and later as a tool for solving partial differential equations on a weak formulation. The Finite Element Method makes it possible to simulate different scenarios during the development process of a product and therefore it helps the companies to save a lot of time and save money by reducing the experimental testing.

When using FEM for linear elastic analyses, usually a Computer-Aided Design (CAD) model of the structural part is imported into the pre-processor. The imported geometry is in most cases simplified (if it contains very complex curvatures or have parts that are considered to be unimportant for the analysis) and then various kind of elements, see Figure 11, are used in order to discretize the problem. The elements are interconnected at nodes and every node has a certain number of degrees of freedom. Every type of element itself can have various properties, which are strongly dependent on the element formulation.

There are four main groups of elements:

- *Zero-dimensional elements*
- *One-dimensional elements*
- *Two-dimensional elements*
- *Three-dimensional elements*

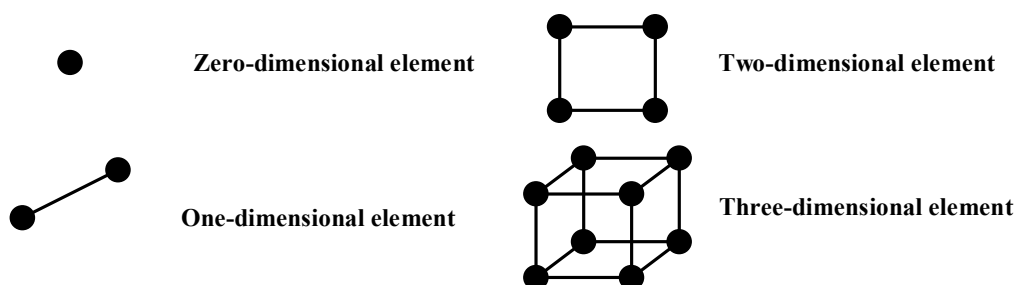


Figure 11: Various types of elements that is available in commercial FE software.

After the problem is discretized with elements and appropriate boundary conditions, the global stiffness matrix is assembled by summarizing the contribution of all element stiffness matrices and then this system of equations are solved for the displacements.

When the displacements are obtained, it is possible to calculate strains and stresses by use of the fundamental equations from Solid Mechanics theory.

3.2 Plate Buckling Theory

There exists a wide literature that describes the plate buckling behavior for various types of plates, subjected to different types of load and with various edge conditions (Brush & Almroth, 1975; Timoshenko & Woinowsky-Krieger, 1959).

The definition of the critical load of a structure is where it loses its stability. An analytical calculation of the critical buckling load by use of the theory elasticity can be done in two ways, either by use of an energy method or by solving the differential plate equation. The plate differential equation looks as follows (Brush & Almroth, 1975):

$$\frac{\partial^4 w(x, y)}{\partial x^4} + 2 \frac{\partial^4 w(x, y)}{\partial x^2 \partial y^2} + \frac{\partial^4 w(x, y)}{\partial y^4} = \frac{12(1 - \nu^2)}{Et^3} \left(N_x \frac{\partial^2 w(x, y)}{\partial x^2} + 2N_{xy} \frac{\partial^2 w(x, y)}{\partial x \partial y} + N_y \frac{\partial^2 w(x, y)}{\partial y^2} \right) \quad (1)$$

If a perfectly flat, rectangular plate that is simply supported along all four edges and subjected to a uniaxial compressive force N_x in the x-direction, without any initial imperfections is considered, then the equilibrium equation takes the following form:

$$\frac{\partial^4 w(x, y)}{\partial x^4} + \frac{\partial^4 w(x, y)}{\partial x^2 \partial y^2} + \frac{\partial^4 w(x, y)}{\partial y^4} = \frac{12(1 - \nu^2)}{Et^3} \left(-N_x \frac{\partial^2 w(x, y)}{\partial x^2} \right) = \frac{1}{D} \left(-N_x \frac{\partial^2 w(x, y)}{\partial x^2} \right) \quad (2)$$

where $w(x, y)$ is the out-of-plane deflection and D is the flexural rigidity. The out-of-plane deflection, $w(x, y)$, can be described by a double sine function Fourier series:

$$w(x, y) = \sum_{m=1,2,3} \sum_{n=1,2,3} w_{mn} \sin \frac{m\pi x}{a} \sin \frac{n\pi y}{b} \quad (3)$$

where m and n indicate the number of half sine waves in the two directions over the plate. This assumed sine function describing the out-of-plane deflection automatically satisfies the boundary conditions for a simply supported plate, as there are no deflections and bending moment (curvatures) at $x = 0$, $x = a$ and $y = 0$, $y = b$ respectively.

If the equation for the out-of-plane deflection is inserted into Equation (2), the following expression is obtained:

$$\left(\frac{m^4 \pi^4}{a^4} + \frac{2m^2 n^2 \pi^4}{a^2 b^2} + \frac{n^4 \pi^4}{b^4} \right) = \frac{12(1 - \nu^2)}{Et^3} N_{xcr} \frac{m^2 \pi^2}{a^2} \quad (4)$$

Rearranging Equation (4) then gives the following expression for the critical load:

$$N_{xcr} = \frac{\pi^2 Et^3}{12(1 - \nu^2)} \frac{\left(m^2/a^2 + n^2/b^2 \right)^2}{m^2/a^2} = \frac{\pi^2 Et^3}{12(1 - \nu^2)} \left(\frac{m}{a} + \frac{n^2 a}{mb^2} \right)^2 \quad (5)$$

The lowest value of the buckling load is obtained for $n = 1$:

$$(N_x)_{cr} = \frac{\pi^2 Et^3}{12(1 - \nu^2)b^2} \left(m \frac{b}{a} + \frac{a}{mb} \right)^2 \quad (6)$$

The critical buckling stress is obtained by dividing Equation (6) with the thickness of the plate:

$$\sigma_{cr} = \frac{N_{x_{cr}}}{t} = \frac{\pi^2 E t^2}{12(1-\nu^2)b^2} \left(m \frac{b}{a} + \frac{a}{mb} \right)^2 \quad (7)$$

$$\sigma_{cr} = \frac{\pi^2 E}{12(1-\nu^2)} \frac{t^2}{b^2} \left(m \frac{b}{a} + \frac{a}{mb} \right)^2 = \frac{\pi^2 E}{12(1-\nu^2) \left(\frac{b}{t} \right)^2} \left(m \frac{b}{a} + \frac{a}{mb} \right)^2 \quad (8)$$

Simplifying Equation (8) by introducing the expression for the buckling coefficient:

$$K = \left(m \frac{b}{a} + \frac{a}{mb} \right)^2 \quad (9)$$

The final expression for the critical buckling stress looks as follows:

$$\sigma_{cr} = K \frac{\pi^2 E}{12(1-\nu^2) \left(\frac{b}{t} \right)^2} \quad (10)$$

For analysis of a simply supported plate including material nonlinearity such as plasticity, the equation takes the following form according to the Strength Data Handbook of Saab:

$$\sigma_{cr} = K \frac{\pi^2 E \sqrt{\eta}}{12(1-\nu^2) \left(\frac{b}{t} \right)^2} \quad (11)$$

where $\eta = E_t/E$ is a reduction factor and where E_t and E are the tangent modulus and the Young's modulus respectively. Also for some loading cases, the tangent modulus is replaced by the secant modulus, E_s , instead.

The buckling coefficient varies with the aspect ratio and also with the number of half waves over the length of the plate, m , which can be seen in Figure 12. Plates that are loaded in uniaxial compression have different values of the buckling coefficient if for example compared against a plate subjected to in-plane shear load.

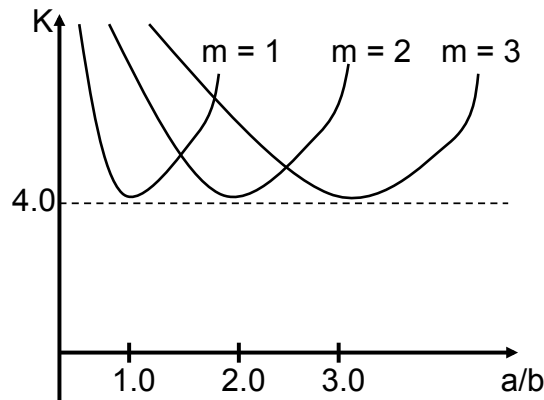


Figure 12: The buckling coefficient, K , varies with the number of half waves. For very slender plates, the value of the buckling coefficient starts to converge.

3.3 Buckling and Finite Element approach

3.3.1 Fundamentals of Buckling Analysis using FEM

According to Campbell et al. (1993) and Lee (2001) the procedure from an FE point of view when performing buckling analysis of a structure consists of three steps. First, a linear buckling analysis is performed. Cook et al. (2002) describes the linear buckling analysis as an eigenvalue problem whose smallest root defines the smallest level of external load for which there is bifurcation i.e. where two equilibrium paths intersect.

The eigenvalue problem looks like the following:

$$([K] + \lambda_{cr}[K_{\sigma}]_{ref})\{\delta u\} = 0 \quad (12)$$

where $[K]$ is the stiffness matrix, λ_{cr} is the eigenvalue, $[K_{\sigma}]_{ref}$ is the stress stiffness matrix and $\{\delta u\}$ is the eigenvector. The magnitude of the eigenvector is normalized in a linear buckling analysis problem meaning that it defines the shape of the eigenmode but not the amplitude. The linear buckling analysis consists of two subcases. In the first subcase the load is applied and in the second subcase, the eigenpairs are calculated using an extraction method e.g. the Lanczos method or the Subspace method.

According to Bathe (2012), both the Subspace method and the Lanczos method are the two widely used schemes which both have different capabilities and attractive properties. The Subspace iteration method is very robust but the speed is dependent on the starting subspace while the Lanczos method is very effective in the case when solving for many eigenpairs.

Generally, the buckling load obtained from a linear buckling analysis is higher than the true buckling load of a structure. The reason is that there are no imperfections included in a linear buckling analysis, which are present when doing experimental testing.

The nonlinear buckling analysis is a simulation procedure that allows for large deformations and geometrical and/or material nonlinearities. This type of analysis is the second step after a linear buckling analysis approach.

There are three main types of nonlinearities:

- *Material nonlinearity*, in which material properties are functions of stress or strain.
- *Contact nonlinearity*, in which gaps between parts can open/close or the contact area between adjacent parts change.
- *Geometric nonlinearity*, in which deformations are large enough to make the small displacement assumption invalid.

In nonlinear analysis, the stiffness matrix $[K]$ and/or the load vector $\{f\}$ in the structural equations, $[K]\{u\} = \{f\}$, become functions of the displacements, $\{u\}$. This makes it no longer possible to solve the systems of equations directly for the displacements by inverting the stiffness matrix. Consequently, a tangent stiffness matrix, $[K]_t$, is created, which includes both the effect of changing geometry as well as stiffening due to stress. The procedure then becomes to solve $[K]_t\{\Delta u\} = \{\Delta f\}$ by use of an incremental scheme, e.g. the Newton-Raphson method, see Figure 13.

According to Cook et al. (2002) the Newton-Raphson method is the most rapidly convergent process and has a quadratic convergence rate and is also the most commonly implemented solution scheme in commercial FE software.

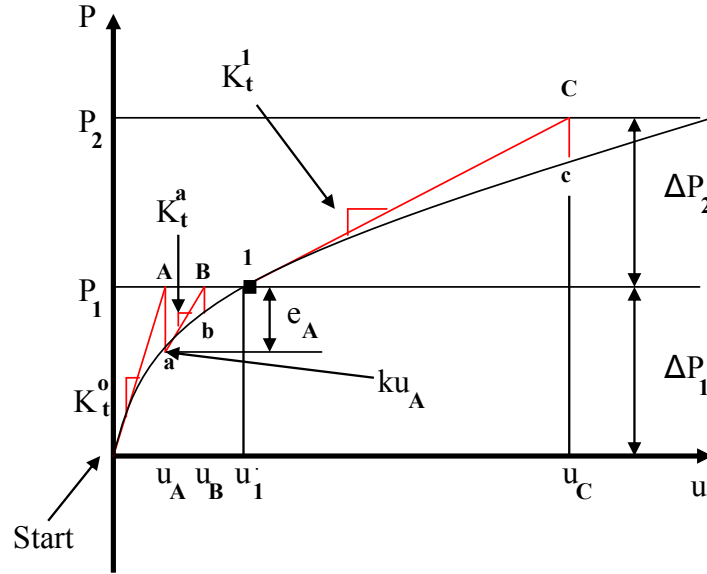


Figure 13: The Newton-Raphson iteration scheme.

When performing nonlinear buckling analysis of plates, the usually used geometrical models in the simulations are perfectly flat plates, where all nodes are in the same plane. Consequently, the plates will not buckle without putting in some small imperfection in the structure. In reality, there are no plates that are produced perfectly flat without any defects and this has to be taken into account when creating FE models of this nature.

There are several ways of modeling imperfections e.g. sometimes a small out of plane force or translation of some nodes in the normal direction of the plate is sufficient in order to excite the first eigenmode. The most common and structured way to model imperfections is to use the pattern for the first eigenmode (under the assumption that this is the true shape of the buckling mode), obtained from the linear buckling analysis.

First, the solver runs through a linear buckling analysis where it collects and scales the chosen eigenmode, then it is used as an initial displacement pattern for the corresponding nodes in the nonlinear buckling analysis, which is performed in the second run. See Figure 14 for a schematic overview of the process. There is also a possibility to use a superposition of a couple (or as many as wanted) of the eigenmodes, where usually the largest magnitude is given the first mode because the structure will most likely buckle in this way.

The imperfections have the following form in Abaqus (Abaqus Version 6.11, 2011):

$$\Delta x = \sum_{i=1}^n w_i \{\phi_i\} \quad (13)$$

where Δx is the magnitude of the imperfection, $\{\phi_i\}$ is the shape of the eigenmode and w_i is the amplitude or scaling factor. MSC Nastran uses the same principle as Abaqus, but the way of applying the imperfection on to the geometry differs between the two FE solvers. In Abaqus, the keyword *IMPERFECTION is available and makes it possible to automatically

chose, scale and apply the imperfection to every node by editing the input file while in MSC Nastran, this must be done manually using its pre-processor.

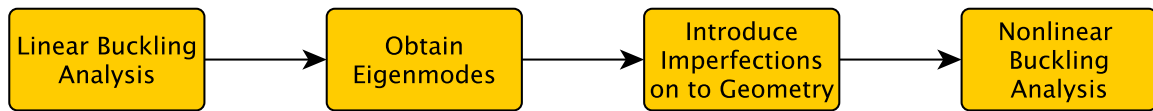


Figure 14: Flowchart describing the procedure of how to obtain and apply imperfections to a FE model.

A major problem in nonlinear buckling analysis is to quantify and motivate the amount of imperfection that has to be included in the analysis. How is it possible to know how large amplitude to use?

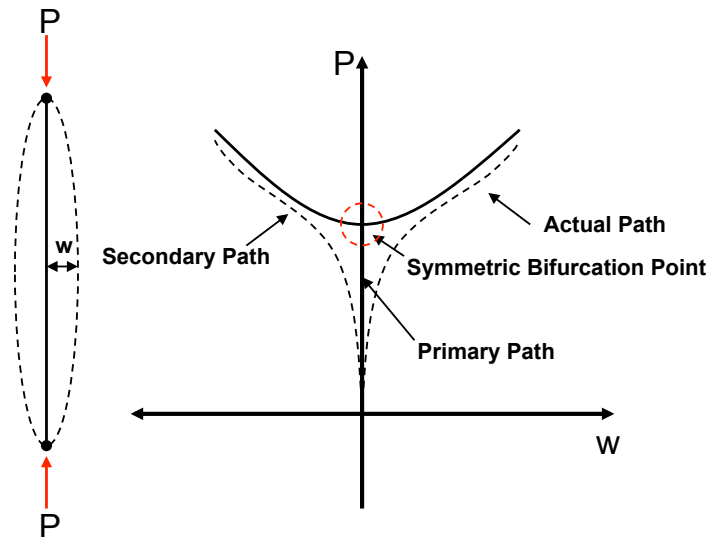


Figure 15: The primary and secondary paths for a perfect plate and the actual part obtained due to imperfections.

In order to answer this question, usually an imperfection sensitivity analysis has to be carried out. The information obtained in the sensitivity analysis makes it possible to quantify how big influence the imperfection has on the buckling load of the structure. If the load versus out-of-plane deflection paths in Figure 15 and Figure 16 are considered, it is possible to see the effect of imperfections in contrast to an ideal buckling path and realise that including imperfections reduces the buckling load of a structure. The path later on converges and coincides with the ideal bifurcation path, in other words the postbuckling path is not affected by the imperfections.

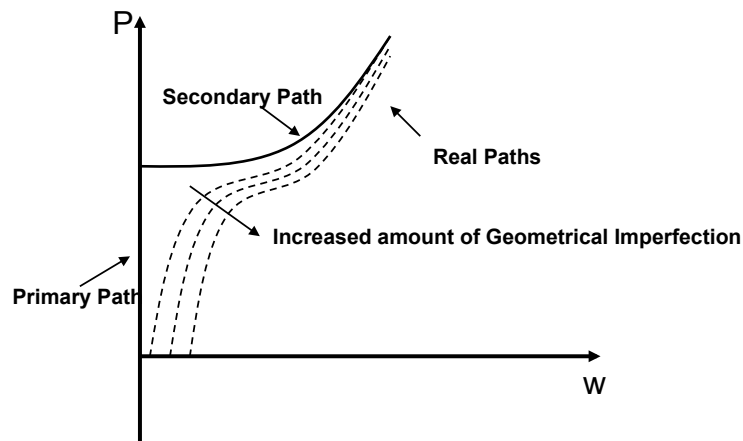


Figure 16: The ideal path (primary and secondary) in contrast to the real path obtained due to presence of imperfections.

A third analysis may be carried out for investigating the postbuckling of the structure. It can be of interest to see if the structure continues to carry the load after it has reached its critical limit or if it loses all its stiffness and collapses.

When investigating the postbuckling, the used iteration scheme is called the Riks method and is a variant of the Arc Length method¹. Unlike the Newton-Raphson method, this method puts in an extra constraint when iterating for the solution and this constraint allows the solver to lower the applied load and find equilibrium. This property of the Riks method makes it possible to trace the behavior after a limit point is reached, even though that the stiffness matrix is not positive definite.

According to Abaqus manual (Abaqus Version 6.11, 2011), the loading during a step in the Riks solution scheme is always proportional to the current load magnitude:

$$P_{tot} = P_0 + \zeta(P_{ref} - P_0) \quad (14)$$

where P_0 is the dead load, P_{ref} is a reference load and ζ is the Load Proportionality Factor (LPF).

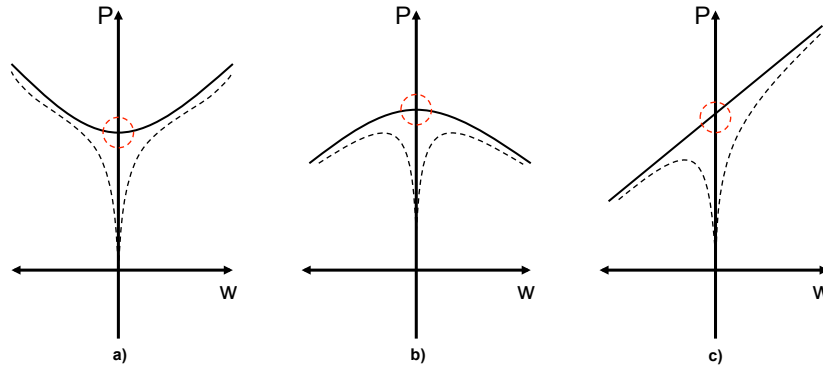


Figure 17: Different types of buckling and postbuckling paths; a) Stable postbuckling, b) Unstable postbuckling and c) Stable/Unstable postbuckling.

Postbuckling can be divided into two different types. The first type is called stable postbuckling and the second is called unstable postbuckling. The characteristic of stable postbuckling behavior is when the structure continues to carry the load that it is subjected to and keep its stiffness or in FE terms explained as having a positive definite stiffness matrix, see Figure 17a.

The definition of unstable postbuckling is when the structure loses its stiffness and is no more able to carry the same amount of load. This often leads to that the structure starts to undergo very large geometrical changes for decreased or unchanged loading, see Figure 17b.

¹ The Newton method can also work as a solution scheme when doing postbuckling analysis but only with the requirement that the postbuckling path is stable. This is hard to know in advance, so therefore the Riks method is recommended for this kind of analysis because it is valid for both stable and unstable behavior of the postbuckling paths.

3.3.2 Estimation of Buckling load in Nonlinear Analysis

When performing a nonlinear buckling analysis, the load is applied to the nodes in increments using the LPF and then a force versus out-of-plane displacement curve is obtained. From this curve, it is possible to find out for which load, P , the out-of-plane displacement, w , increases rapidly, i.e. the structure buckles. At this point the load goes from P to P_{cr} , which is the force utilized when calculating the buckling load of the structure.

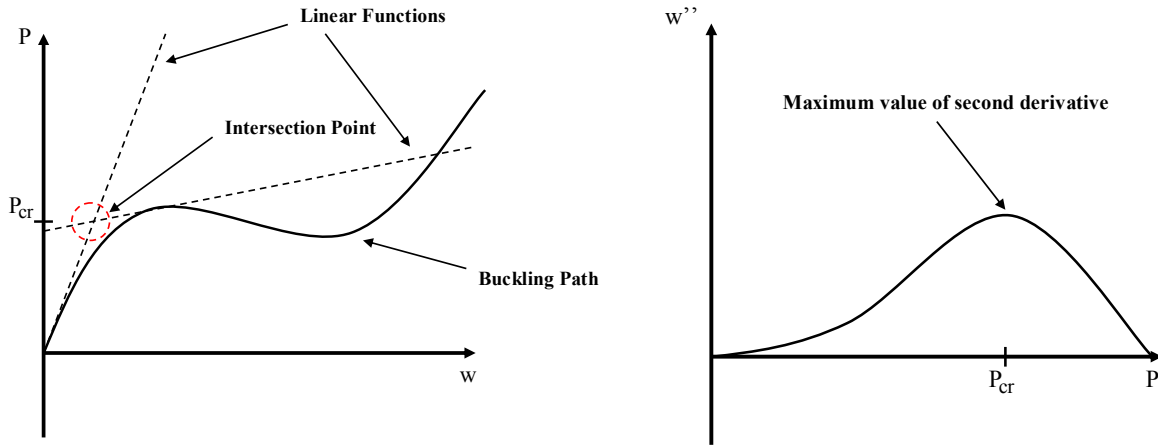


Figure 18: The Linearization method (left) and the Second derivative method (right), both utilized for estimating the buckling load in nonlinear buckling analysis.

For some load cases or geometries, the buckling process can be somewhat diffuse and not occur so rapidly, which makes it hard to concretize the buckling load. Consequently, there are some methods that can be utilized for estimating the critical buckling load in nonlinear analysis and in this thesis, two different approaches are tested and evaluated against each other.

The following two methods are evaluated:

- *The Linearization method*, in which the idea is to create two linear functions, one that starts from the origin and follows the slope of the prebuckling force path versus out-of-plane displacement curve and another one that follows the postbuckling slope path, i.e. where the path shows a great increase in displacement for a small increase of the load. The intersection point between these two linear functions then gives the estimated critical buckling load, see Figure 18.
- *The Second derivative method*, where a curve fitting or linearization between the points has to be made with respect to the obtained force versus out-of-plane displacement curve from the nonlinear analysis. In this thesis, for this particular method, the force is plotted on the x-axis and the out-of-plane displacement on the y-axis. After an equation describing the out-of-plane displacement versus force curve is obtained from the curve fitting, it is differentiated two times with respect to the force and then values of this function is calculated for all load increments. Mathematically, at the load increment where the largest value of the second derivative is obtained is the corresponding part where the largest curvature is obtained on the original out-of-plane displacement versus force curve, which is also where buckling occurs. This can be seen in Figure 18.

Both of the methods contain a lot of approximations and are strongly dependent on the quality of the nonlinear solution, especially the second derivative approach because of the curve fit step where it can be quite complicated to make a good approximation if the structure shows an unstable postbuckling path.

Using the linearization method can result in a bit arbitrary approximations depending on the defined slopes of the linear functions and this method is also a bit sensitive to where the second function is chosen to cross the y-axis.

3.3.3 Estimation of Error

The method used for calculating the error when two cases are evaluated against each other is an absolute relative error method, which is calculated by subtracting the difference between the two results and dividing by the value that is constant and compared against.

The following equation is used for estimating the absolute relative error with respect to the buckling load obtained numerically versus the handbook result:

$$error = \left| \frac{\sigma_{cr}^{NUMERICAL} - \sigma_{cr}^{THEORETICAL}}{\sigma_{cr}^{THEORETICAL}} \right| \quad (15)$$

CHAPTER 4

LITTERATURE SURVEY

This chapter contains overall information about what has been done earlier with respect to application of the Finite Element Method in the field of Buckling in Plates under various geometries, types of load and boundary conditions.

As mentioned in the introduction, aircraft structures in service are exposed to a large amount of cyclic loads, i.e. during take off, landing and therefore also subjected to thousands of buckling cycles. Buckling is an instability phenomenon that can lead to very sudden loss of stiffness in a structure and therefore cause catastrophic results. Timoschenko (1936) utilized an energy method to study the buckling behavior of rectangular plates subjected to in-plane shear load. He only considered the symmetrical buckling mode, which caused an error in the prediction of the critical buckling load of the plate. Unlike Timoschenko (1936), Stein and Neff (1947) considered both symmetric and asymmetric buckling modes, which resulted in a correct evaluation.

The increased use of numerical methods, i.e. the Finite Element Method (FEM) for studying the buckling behavior of plates has led to increased research within this field. Under what conditions is it possible to correctly capture the buckling behavior of plates? What are the key parameters that need to be considered when using numerical methods such as FEM for predicting the buckling load of a structure?

A lot of research has been done with respect to buckling of plates with different kinds of geometries (stiffened plates, plates with/without reinforced holes, various aspect and slenderness ratios), types of loading (uniform compression, in-plane shear load, loads that act out of the plane or any other combination of these), materials (isotropic material, anisotropic material, orthotropic material), boundary conditions (clamped, simply supported, free edges or any other combination) and complexity of the analysis (linear, nonlinear and elastic, nonlinear and plastic).

If a plate is loaded beyond its critical buckling load, the postbuckling behavior takes place. In some dimensioning criteria's, structures are allowed to buckle, as long as it is in the elastic region for the material and then the postbuckling response can be of interest to study. Some structures continue to carry load after buckling, i.e. they show stable postbuckling paths while others can lose stiffness, i.e. show unstable postbuckling paths.

According to Abaqus and MSC Nastran manuals (Version 6.11, 2011; Version 2012.2, 2012), the recommended mesh density to use when performing buckling analysis in order to catch the correct behavior is approximately four elements per half wave, if four node shell elements are used for discretizing the problem. This implies that the needed mesh density will differ with the used boundary conditions. In reality, the conditions are neither simply supported nor clamped but something in between these two.

Soh et al. (2000) have performed elasto-plastic buckling analysis of simply supported plates subjected to uniaxial compression load. The aim of the work was to determine the buckling

load of three different types of plates made out of composite material. The obtained numerical results showed good correlation when compared to the experiments.

Gheitasi and Alinia (2010) investigated the affect of slenderness ratio on metal plates subjected to in-plane shear load. Slenderness ratio is used to describe the ratio between the width and thickness of the plate while the slenderness parameters also involves the yield stress and Young's modulus of the material:

$$\beta = \frac{b}{t} \quad (16)$$

$$\lambda = \beta \sqrt{\frac{\sigma_y}{E}} \quad (17)$$

where β is the slenderness ratio, b is the shortest side of the plate, t is the thickness, λ is the slenderness parameter, E is the elastic Young's modulus and σ_y is the yield stress.

Plates can be divided into three groups depending on geometrical dimensions; slender, moderate and stocky. The authors concluded that for slender plates with $\lambda \geq 6$, elastic buckling loads predicted numerically using the Finite Element Method are in total agreement with those obtained from theory. Slender plates buckle at lower loads and bifurcate mainly due to geometrical instability within the elastic limits of the material. Stocky plates, where $\lambda \leq 4.5$, show a material bifurcation i.e. they buckle in an inelastic way closer to the yield limit implying that a linear buckling analysis approach is not sufficient to catch the buckling behavior.

According to the research presented by Alinia et al. (2012) the buckling of stocky plates are followed by an unstable postbuckling path meaning no further load carrying capacity. In the other hand, slender plates show a load carrying capacity up to the ultimate load after the buckling load is reached.

Simply supported plates under in-plane shear load with landings (or reinforcements) have been investigated earlier at Saab Aeronautics (LN-017497, 2014) and one of the main conclusions was that the placement of the landing (symmetric or asymmetric) did not affect the buckling load of the plate.

If a structure is very sensitive to imperfections, applying too large amplitude can lead to very conservative results. Also, if a superposition of a few eigenmodes is used, applying to large amplitude on the wrong eigenmode can significantly affect the buckling behavior of a structure. Featherston (2001) showed in his study that increasing the amplitude of the imperfection reduced both the prebuckling stiffness and the buckling resistance of the plate. He also noted in his study that the effect of initial imperfection amplitude is minimal on the postbuckling behavior and the use of the first eigenmode as imperfection did not in any case give the most conservative result.

Plates containing openings is an area in which a lot of research has been done. Pellegrino et al. (2009) examined the linear and nonlinear buckling behavior of plates made out of steel with two types of holes. The plates were exposed to in-plane shear load and the influence of parameters such as dimension, position, shape (circular or rectangular) was investigated. In the study, a strong influence of the hole dimension on the shear buckling coefficient was noted for both circular and rectangular holes.

Shannmugam and Tahmasebinejad (2011) also studied plates containing holes and they concluded that plates with circular holes have higher ultimate load carrying capacity compared to plates with square holes, which implies that circular holes should be preferred to rectangular ones.

Narayan and Chow (1984) investigated the buckling behavior of simply supported and clamped plates containing holes and under uniaxial/biaxial compression or in-plane shear load. They examined parameters such as eccentricity, diameter of the hole and found out that for uniaxially compressed plates, the buckling coefficient is unaffected by the hole location for holes smaller than $d/b \leq 0.2$. For larger holes ($d/b \geq 0.4$), it was observed that for clamped boundary conditions the buckling coefficient decreases as the eccentricity increases, while it decreases more rapidly as the eccentricity increases for simply supported conditions.

The observations made by the authors for a plate with a hole in the tension diagonal subjected to in-plane shear load was that for very small holes ($d/b \leq 0.1$), the buckling coefficient is unaffected up to large eccentricities. For large eccentricities, it starts to increase for clamped boundary conditions while it remains constant for simply supported. When larger holes are considered, the buckling coefficient decreases as the eccentricity of the hole increases.

If the hole is placed in the compression diagonal, the results differ if compared to uniaxially compressed plates. For small holes ($d/b \leq 0.1$), the buckling coefficient is not affected by the placement of the hole but it increases as the eccentricity becomes larger for holes that fulfill the condition $d/b \geq 0.2$. The same results are obtained for both rectangular and circular holes and not affected by the choice of boundary conditions.

Because of the great reduction in buckling load when considering a hole in plates, various methods for how to increase the buckling resistance have been examined in the past. In 1949, W. D. Kroll (1949) published his article where simply supported plates loaded in in-plane shear containing reinforced holes were examined. He concluded that even though a very big reduction of the buckling load is obtained when a hole is considered in a plate, it is possible to increase the buckling resistance by the use of reinforcement.

Further, Cheng and Zhao (2010) investigated the effects of four types of stiffeners in plates containing holes. The plates were subjected to uniaxial compression load and the types of stiffeners investigated were ringed stiffener, flat stiffener, longitudinal stiffener and transverse stiffener. It was found out by the authors that the buckling behavior of plates with reinforced holes are similar to those with unreinforced ones but the buckling and ultimate load of all plates containing holes are improved due to the stiffeners. The ringed and flat stiffener gave the best results in elasto-plastic ultimate strengths for thick plates ($b/t \leq 40$), while the greatest increase in elasto-plastic ultimate strengths and elastic buckling loads for thin plates ($b/t \geq 80$) were achieved by the use of longitudinal stiffeners.

CHAPTER 5

FE Modeling

This chapter describes the main part of the work performed and it starts with describing the used software and some general knowledge about how to setup a FE analysis, then it continuous to describe all the FE models that were used in the simulations.

5.1 General

The procedure of setting up an FE model using a pre-processor is very straightforward. First, the pre-processor program is selected and then the desired geometry is modeled. After the desired geometry is obtained, the surface is meshed with the proper type of element. When satisfied with the mesh, appropriate boundary conditions and loads are applied to the model. Further on, depending on what kind of an analysis that is going to be performed and the desired output variables, corresponding control cards have to be selected.

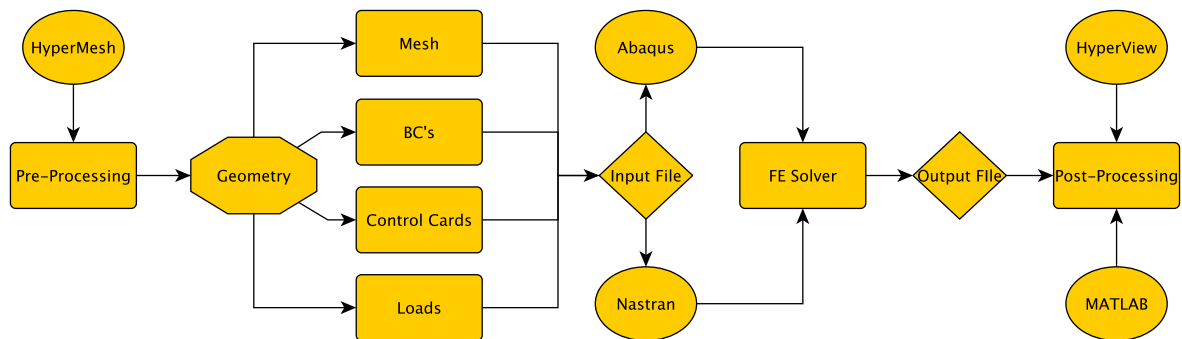


Figure 19: Flowchart describing how to set up an FE structural analysis.

After this is done, the pre-processor compiles and exports the FE data as a bulk data file, which is then submitted into the selected FE solver. After solving the problem, the FE solver generates an output file that contains the results from the analysis. This output file is then used as input to the post-processing program, which is used for formatting and presenting the results in a desired way. See Figure 19 for a schematic overview of the process describing how to setup an FE analysis.

5.1.1 Solver

There exist a large amount of FE software, both in open source and commercial. In this thesis, the two solvers MSC Nastran (SOL101 together with SOL105 for linear static buckling analysis and SOL106 for nonlinear analysis) and Abaqus have been used.

5.1.2 Pre- and post processors

Also with respect to pre- and post processors, there exists a wide variety of different software to choose between. In this thesis, the HyperWorks 12.0 package by Altair Engineering containing HyperMesh and HyperView was utilized for setting up the problems and viewing the results. Finally, the software MATLAB R2012a was used for handling data and plotting graphs.

5.1.3 Boundary conditions and Load types

The type of boundary condition used for the largest part of the models is simply supported conditions, but for the convergence study with respect to the mesh, also clamped conditions were studied.

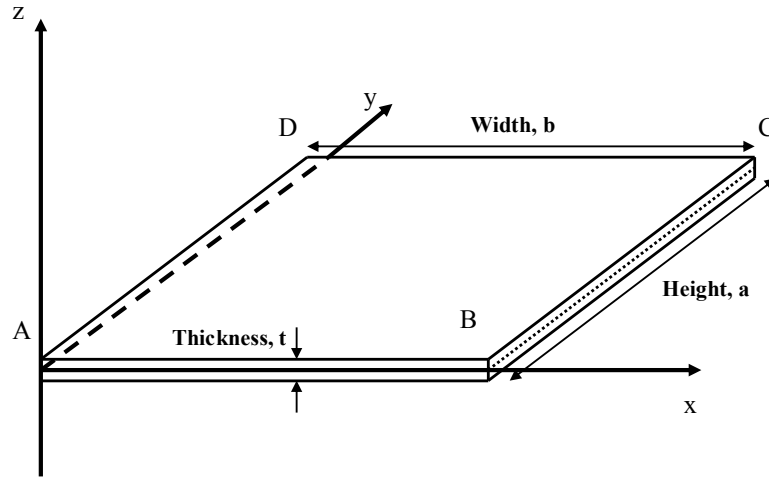


Figure 20: Definition of the different geometrical parameters and the coordinate system.

In reality, neither simply supported nor clamped conditions are sufficient to describe the behavior of a structure because the mobility is something in between these two. If the plate is modeled according to Figure 20 and the coordinate system is oriented in the way, then following the constraints were applied to the structure when simulating simply supported conditions:

Table 1: Definition of the displacement constraints for a simply supported plate where U1, U2, U3 are the translational degrees of freedom and R1, R2, R3 are the rotational degrees of freedom at each node.

FE Modeling	U1	U2	U3	R1	R2	R3
Edge A→B			x			
Edge B→C			x			
Edge C→D			x			
Edge D→A			x			
Point A	x	x	x			
Point B						
Point C		x				
Point D						

The corresponding constraints for simulating a clamped plate were the following:

Table 2: Definition of the displacement constraints for a clamped plate where U1, U2, U3 are the translational degrees of freedom and R1, R2, R3 are the rotational degrees of freedom at each node.

FE Modeling	U1	U2	U3	R1	R2	R3
Edge A→B			x	x		
Edge B→C			x		x	
Edge C→D			x	x		
Edge D→A			x		x	
Point A	x	x	x			
Point B						
Point C		x				
Point D						

Two different types of load are considered in the FE models, in-plane shear load and uniaxial compression load, see Figure 21. As magnitude, in all of the linear buckling analyses, a unit load is applied to the involved edges. In the nonlinear buckling analyses, the load is applied incrementally and is therefore dependent on the load proportional factor (LPF).

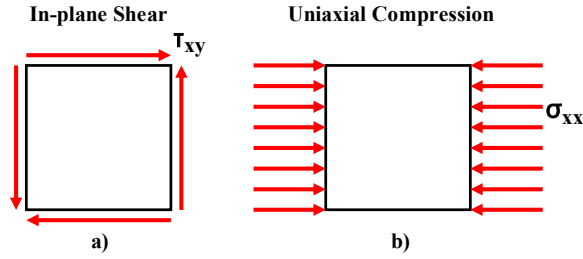


Figure 21: Two types of load are used in the parametric studies; a) In-plane shear load and b) Uniaxial compression load.

5.1.4 Material Data

The material data for linear elastic buckling analysis is presented in the table for each subpart but the material data used in the nonlinear buckling analysis must be calculated manually. The material AL3644-7010 with $E = 71300MPa$, $\nu = 0.33$, $R_m = 490MPa$, $R_{p0.2} = 420MPa$ and Ramberg-Osgood parameter $n = 14$ was used together with the Ramberg-Osgood equation in order to obtain the true stress and strain relationship for the material used during the nonlinear buckling analysis in Part 1 of the thesis. The input for the two used FE solvers differs a bit where MSC Nastran requires the equivalent true strain and stress relationship and Abaqus wants the effective true strain and stress relationship.

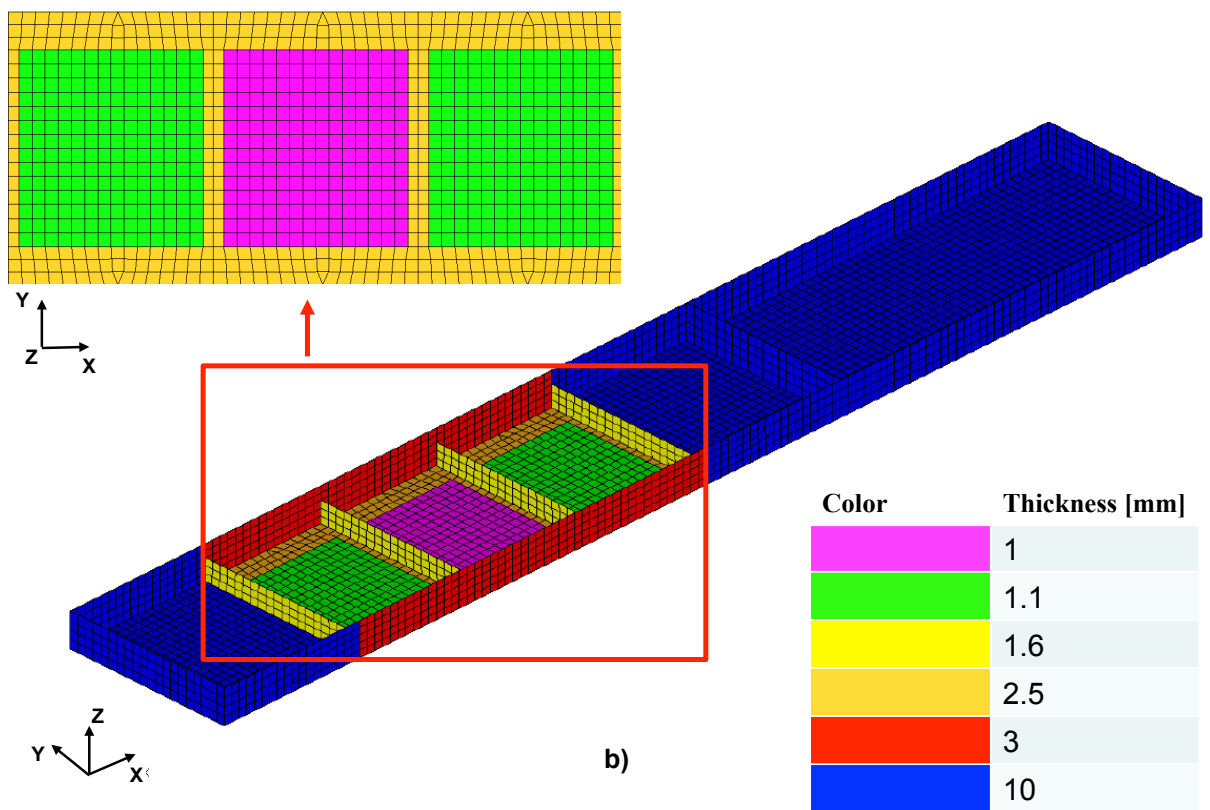
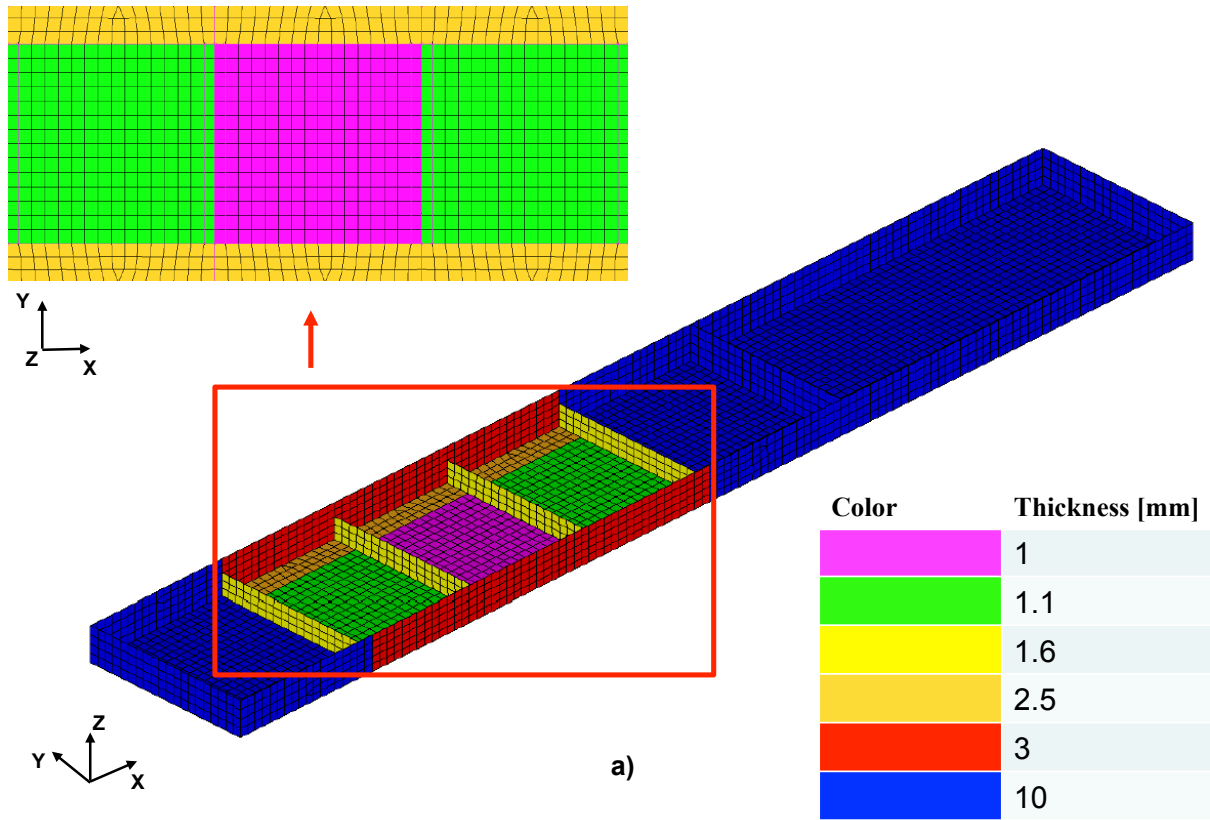
5.2 Part 1

All the FE models used in this part and their geometrical parameters, material properties and FE properties are declared with a corresponding table, containing everything needed to know for recreation, for each subpart. The tables can be found in Appendix A at the end of this report.

Table 3: The subparts in the parametric study and the corresponding table for each case that contains all information with respect to geometry, material and FE properties.

FE Modeling	<i>Model setup parameters</i>
<i>Part 1.1</i>	Table 11
<i>Part 1.2</i>	Table 12
<i>Part 1.3</i>	Table 13
<i>Part 1.4</i>	Table 14
<i>Part 1.5</i>	Table 15
<i>Part 1.6</i>	Table 16
<i>Part 1.7</i>	Table 17
<i>Part 1.8</i>	Table 18

5.3 Part 2



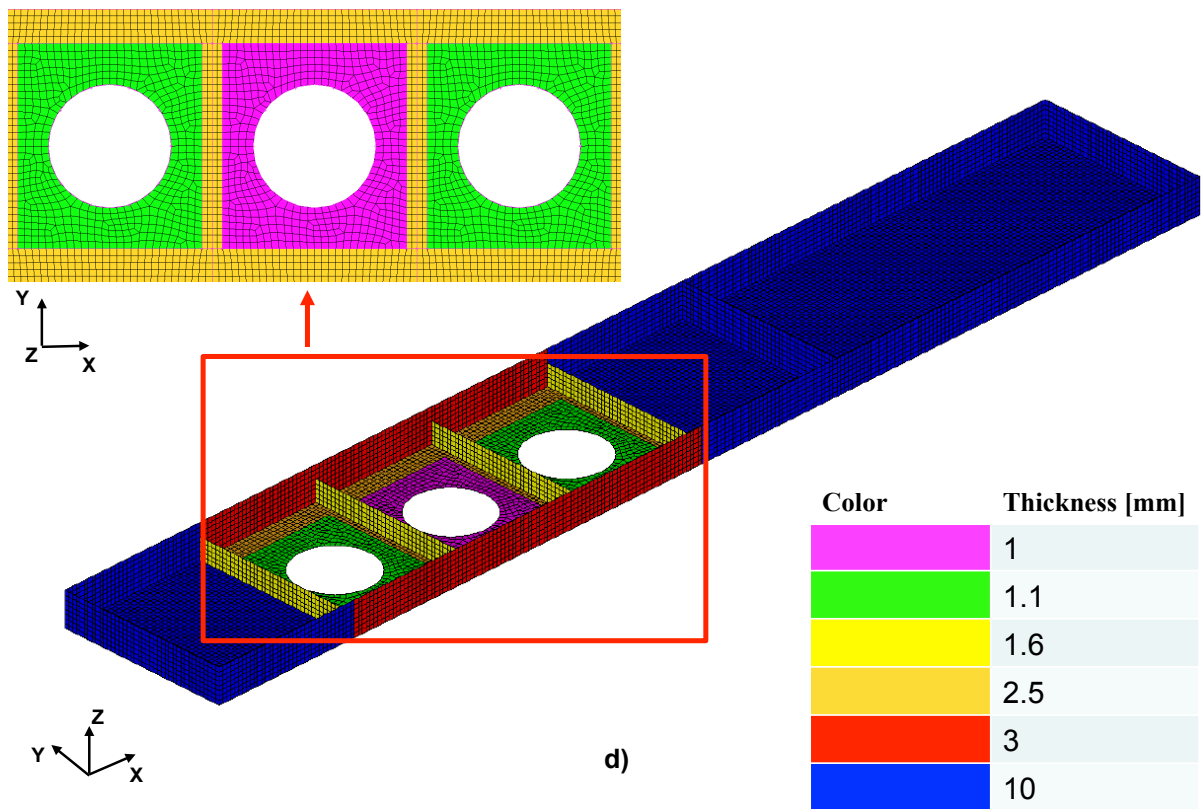
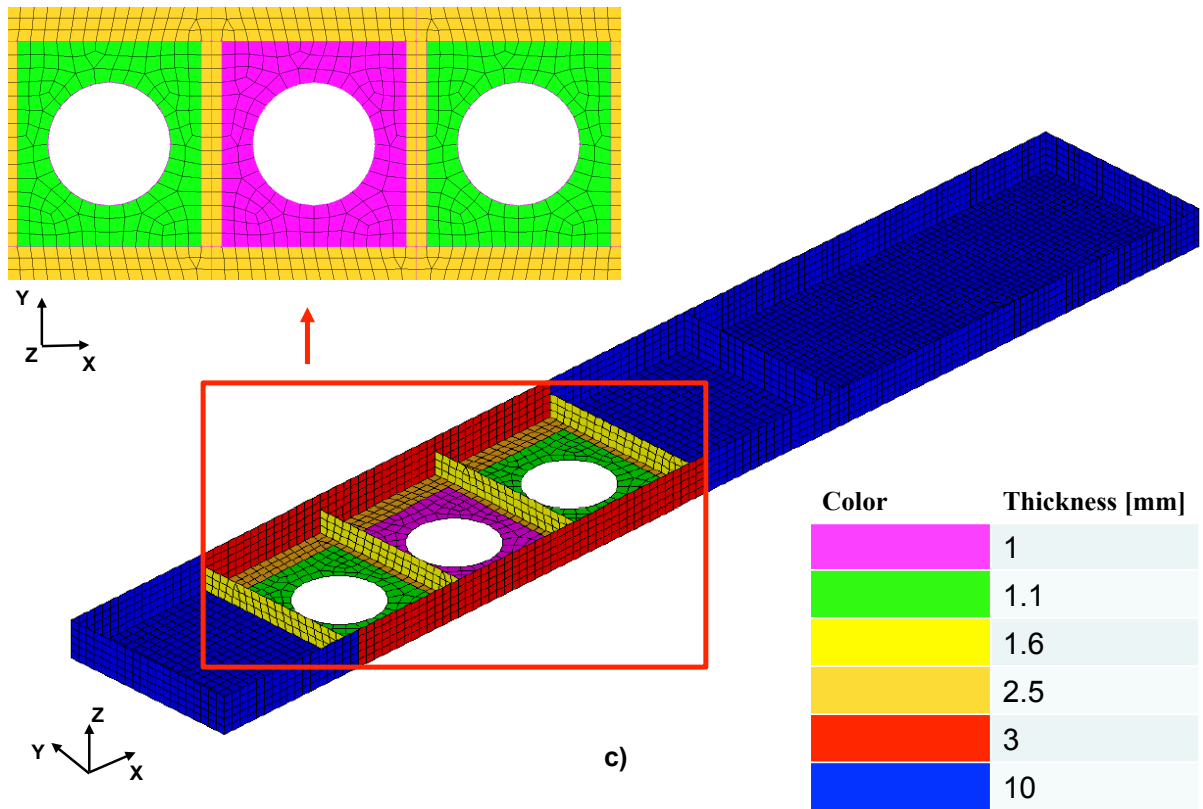


Figure 22: The models are; a) HSM Shear Web Beam Type 1 (previous page), b) HSM Shear Web Type 5 (previous page), c) HSM Shear Web Beam Type 2 and d) HSM Shear Web Beam Type 2 with refined mesh.

5.3.1 Geometry

The geometry of the three models were created according to the drawings in Appendix B, but the bottom radius and milling radius were not taken into consideration because their contribution to the behavior of the beams is assumed to be negligible. The FE models of the various Shear Web Beams can be seen in Figure 22 where there are four different models. The main difference between the models is the variation in the three innermost webs.

The model in Figure 22a has no reinforcement in the webs and is called HSM Shear Web Beam Type 1. The second model is called HSM Shear Web Beam Type 5 and is a model with reinforcement. Last two subfigures (Figure 22c and Figure 22d) shows the same model containing both reinforcement and a hole, but for two mesh densities. Further details with respect to geometry can be seen in Appendix B.

5.3.2 Material data

The material used in the Shear Web Beam is Al3627-06 with $E = 71GPa$, $\nu = 0.33$, $R_m = 490MPa$, $R_{p0.2} = 415MPa$, Ramberg-Osgood parameter $n = 14$ from which then the true stress and strain relationship is obtained using the Ramberg-Osgood equation. The type of analysis used is a nonlinear elastic buckling analysis. According to experiments, buckling occurs before the yield limit in all three cases and at that load, there is no plasticity around the hole, which implies that a nonlinear elastic solution will be sufficient.

5.3.3 Boundary conditions

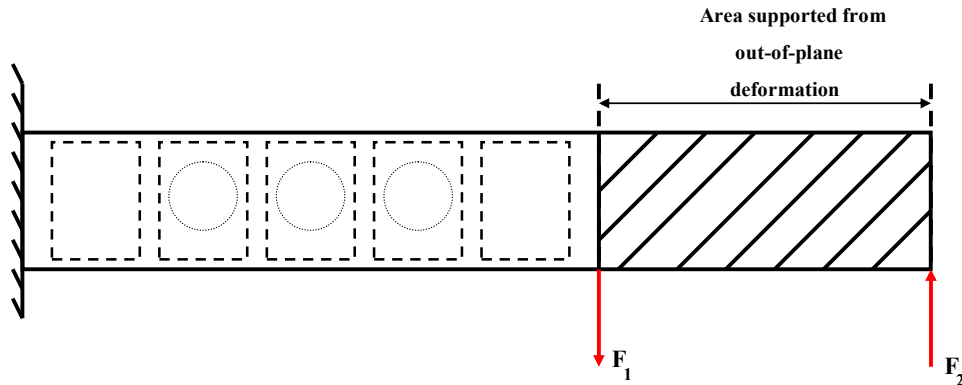


Figure 23: The models are fully clamped on the left side and the part to the right is prevented from out-of-plane deformation.

The same boundary conditions was used in all three FE models, where the Shear Web Beam was clamped at the left side and the part where the load is applied is prevented to move out-of-the plane. The load was applied as two point forces, se Figure 23, for all three different cases with magnitudes according to Table 4. The relationship between the two point forces and calculation of the resultant shear force is according to Saab documentations (FKH-98.119, 1998; JSB3H-09-MP:604, 1998) the following:

$$F_2 = F_1 \frac{420}{870} \quad (18)$$

$$S = F_1 - F_2 \quad (19)$$

Table 4: The load magnitude for each of the test specimens. The load is applied incrementally using 100 load increments during the nonlinear FE simulation of the test.

FE Modeling	100% F_1 [N]	100% F_2 [N]	100% S [N]
<i>HSM Type 1</i>	57618	27818	29800
<i>HSM Type 5</i>	57618	27818	29800
<i>HSM Type 2</i>	30936	14936	16000

The analyses were performed both with and without imperfections. In the case where imperfections were imposed, the first eigenmode for each web was considered, scaled with amplitude of 0.05 or 5%. The Linearization method is used for extraction of the critical buckling load from the buckling paths.

5.3.4 Element type and Mesh

The models were meshed with QUAD4 elements and the typical element density was of 16 elements per half-wave in the areas where buckling is predicted to take place. For the case with increased mesh density, which was investigated for HSM Shear Web Beam Type 2, a mesh consisting of 30 elements per half-wave was used in the areas where buckling is predicted to take place. The reason for this investigation is that the hole is very large, which causes some local buckling effects and to catch this behavior, a finer mesh will be needed around the edge of the hole.

Table 5: The number of elements used in the analyses.

FE Modeling	Standard Mesh	Refined Mesh
<i>HSM Shear Web Beam Type 1</i>	4328 elements	-
<i>HSM Shear Web Beam Type 5</i>	4328 elements	-
<i>HSM Shear Web Beam Type 2</i>	5008 elements	15156 elements

5.3.5 Handbook approach

A simple a handbook method approach is done in order to have some indications on the magnitude of the buckling load. Note that the landings are not taken into account when performing this approach.

Buckling according to SD14-350 for a Plate with Simply Supported edges as for HSM Shear Web Beam Type 5 and Type 1:

$$\frac{a}{b} = \frac{200}{150} = 1.33 \rightarrow K = 7.60 \quad (20)$$

Critical buckling load is calculated according to SD14-115 where $t = t_{min}$:

$$\frac{1}{\sqrt{K}} \frac{b}{t} = \frac{1}{\sqrt{K}} \frac{b}{t_{min}} = \frac{1}{\sqrt{7.60}} \frac{150}{1} = 54.4 \rightarrow S_{cr} = 29.40 * a * t_{min} \quad (21)$$

$$S_{cr} = 29.40 * 200 * 1 = 5.88kN \quad (22)$$

Considering a Plate with a Central Circular hole as for HSM Shear Web Beam Type 2 gives buckling according to SD14-355:

$$\frac{d}{b} = \frac{90}{150} = 0.60 \rightarrow \frac{K}{K_0} = 0.37 \quad (23)$$

Where $K_0 = 7.6$ from previous calculations give now:

$$\frac{K}{K_0} = 0.37 \rightarrow K = 0.37 * 7.6 = 2.81 \quad (24)$$

Once again use SD14-115 in order to find the critical buckling load:

$$\frac{1}{\sqrt{K}} \frac{b}{t} = \frac{1}{\sqrt{K}} \frac{b}{t_{min}} = \frac{1}{\sqrt{2.81}} \frac{150}{1} = 89.48 \rightarrow S_{cr} = 10.90 * a * t_{min} \quad (25)$$

$$S_{cr} = 10.90 * 200 * 1 = 2.18kN \quad (26)$$

Evaluation of experimental critical buckling load for HSM Shear Web Beam of type 1:

$$S_{cr} = 4.77kN \quad (27)$$

Evaluation of experimental critical buckling load for HSM Shear Web Beam of type 5:

$$S_{cr} = 7.05kN \quad (28)$$

Evaluation of experimental critical buckling load for HSM Shear Web Beam of type 2 with a central hole:

$$S_{cr} = 2.40kN \quad (29)$$

Eq. (27)-(29) was taken from the experimental results in Saab testing reports (FKH-98.119, 1998; JSB3H-09-MP:604, 1998).

5.3.6 Experimental testing

Information regarding the testing of the test-specimens, the reader is referred to check the Saab experimental testing reports (FKH-98.119, 1998; JSB3H-09-MP:604, 1998). No further details are described in this thesis except for the test setup, which is illustrated in Figure 24 and pictures in Appendix C.

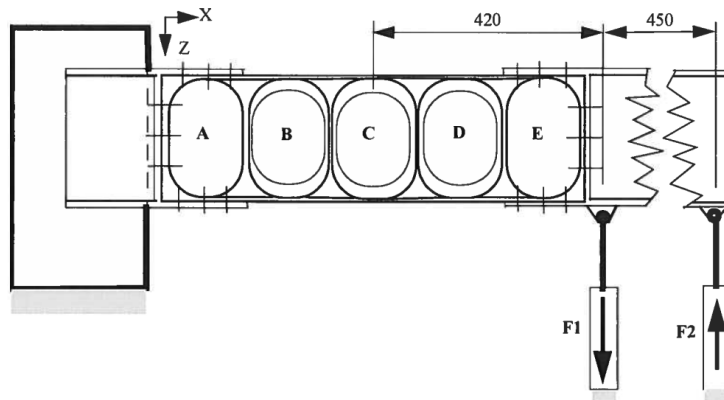


Figure 24: The forces are applied on the HSM Shear Web Beams using two cylinders. Together, the forces generate a resultant shear force that acts on the Shear Web Beam.

CHAPTER 6

RESULTS & EVALUATION

This chapter contains the results that are obtained by the FE models that were presented in the previous chapter. In the beginning of each part, some selected contour plots are presented in order to illustrate the buckling modes for various cases of plates.

6.1 Part 1

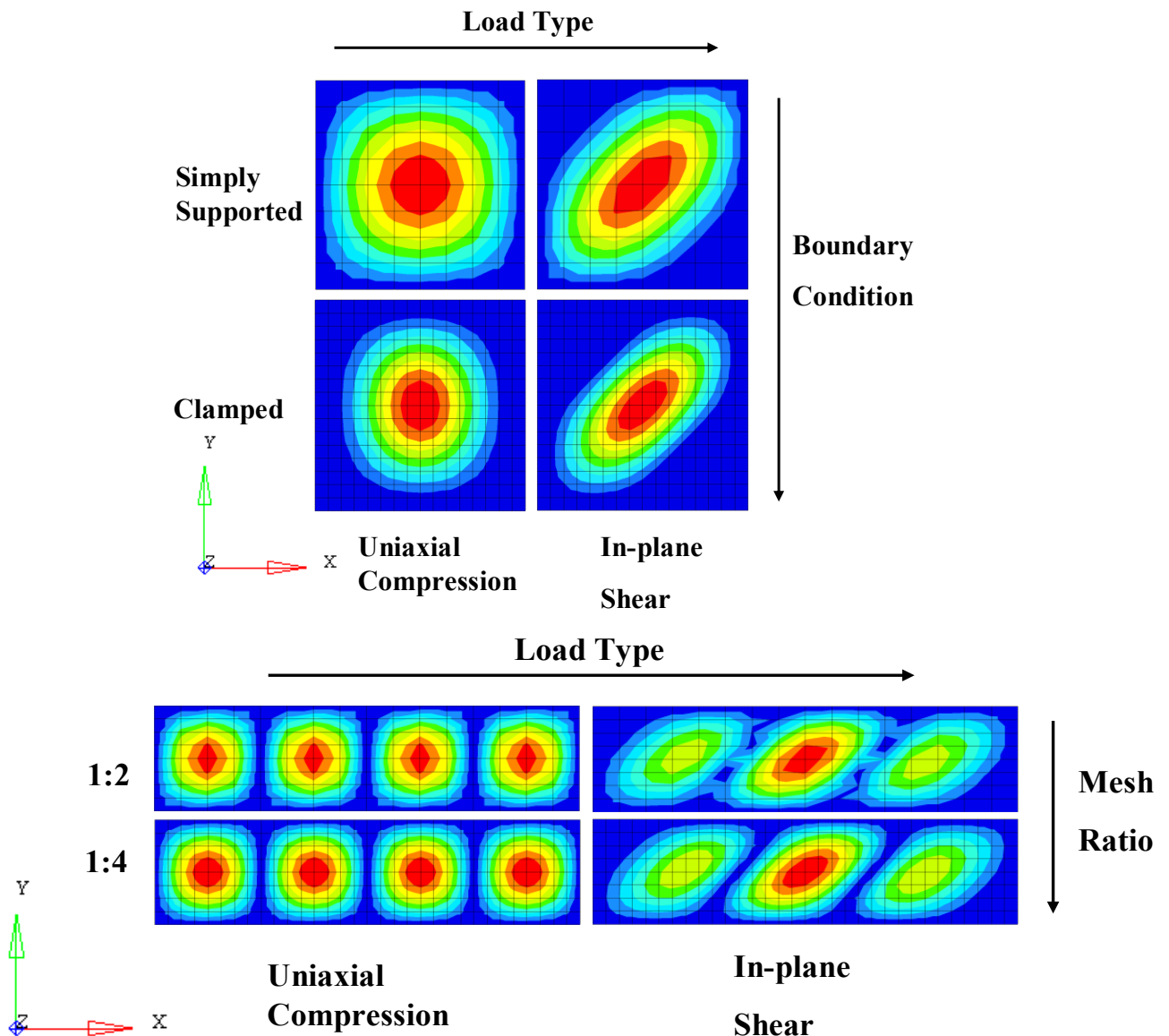


Figure 25: The results for the first eigenmode (z-displacement magnitude) obtained in Part 1.1 where the aim was to perform a mesh convergence study. Top picture shows square plates with two types of loads and boundary conditions and bottom picture shows rectangular plates for two types of loads and mesh ratios.

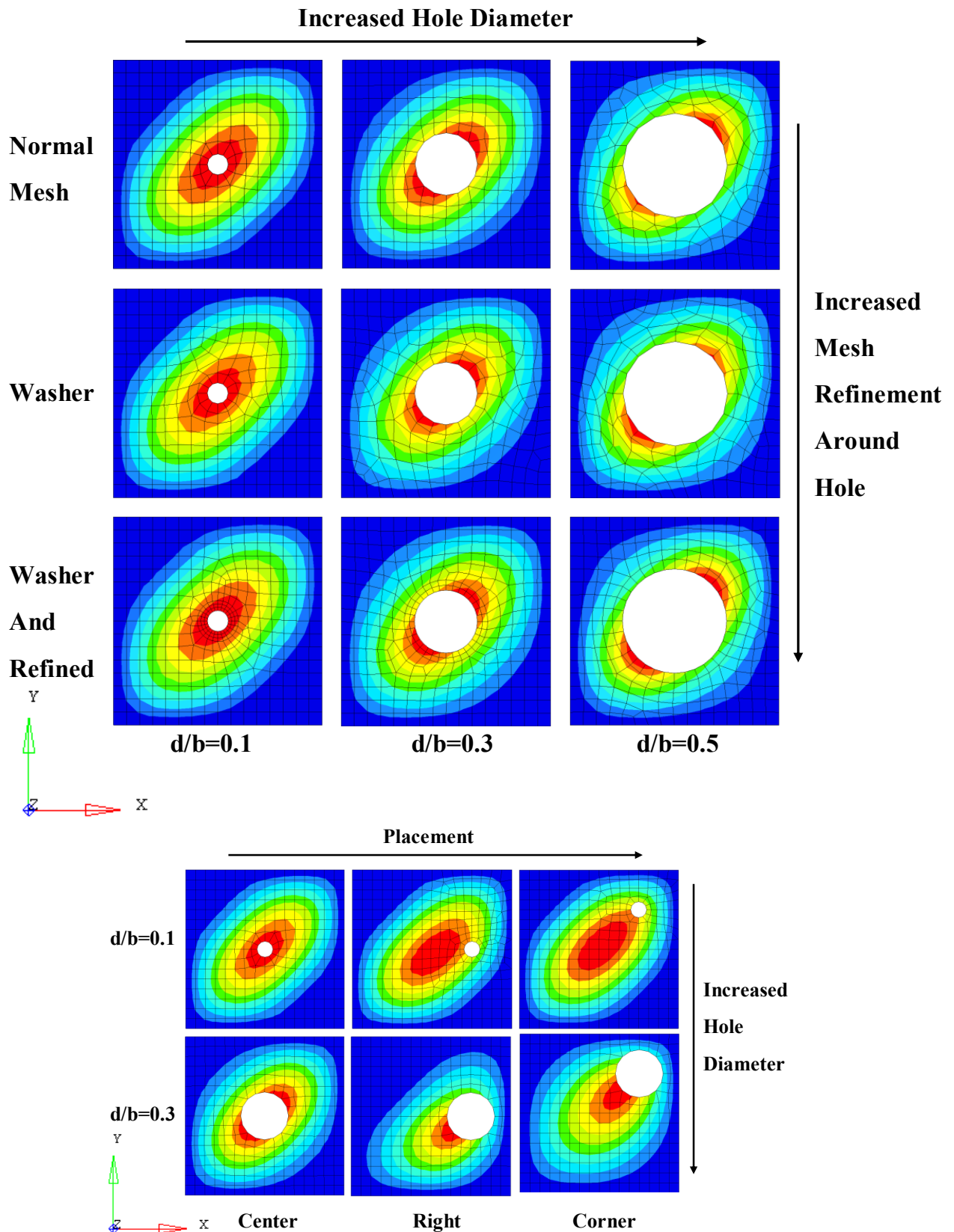


Figure 26: The first eigenmode (z-displacement magnitude) obtained in Part 1.3 where the aim was to linear buckling analysis of plates containing holes. Top picture shows a square plates loaded in in-plane shear where different hole diameters and mesh refinements around the hole were investigated. Bottom picture shows the first eigenmode (z-displacement magnitude) for plates where the placement and hole diameter was investigated

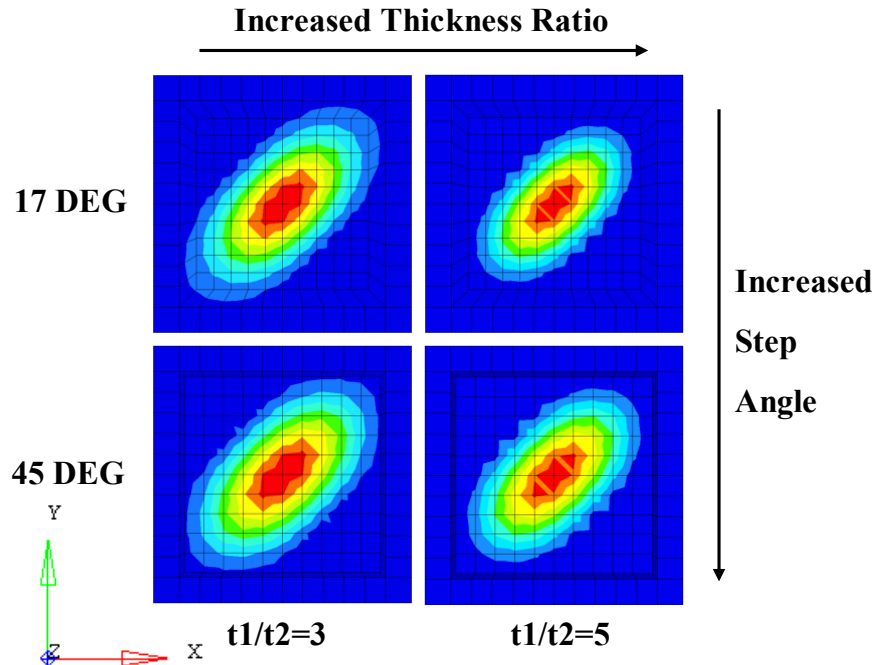


Figure 27: The first eigenmode (z-displacement magnitude) obtained in Part 1.4 where the aim was to perform linear buckling analysis of plates that were modeled containing a step. The picture shows square plates that are loaded in in-plane shear and simply supported along all four edges for two different step angles and thickness ratios.

6.1.1 Part 1.1

The result of the mesh convergence studies performed in the first part of the parametric study is illustrated in Figure 28 to Figure 31. At a first glance, it can be seen that plates loaded in uniaxial compression show faster convergence if compared to plates loaded in in-plane shear. This can be due to that the first buckle mode of compressed plates is shorter and more centered while in the other hand for in-plane shear load, the first buckle mode is longer and across the pressure diagonal of the plate.

An error of 5 % was chosen as a limit of what's acceptable to differ between the numerical results if compared to theory. The recommendations in MSC Nastran and Abaqus manuals are that approximately 4 elements per half wave should be used when performing buckling analysis (Version 6.11, 2011; Version 2012.2, 2012), which is more or less what is obtained for uniaxially compressed plates, see Figure 28.

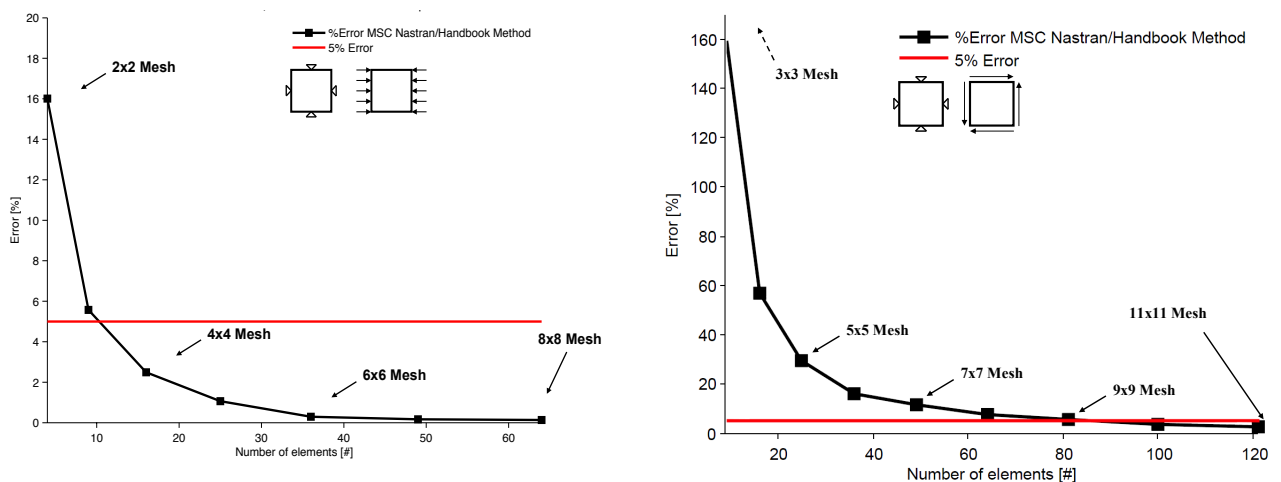


Figure 28: The error between the FE results for plates meshed with 1:1 mesh density and the Saab Strength Data handbook.

If the load type is switched to in-plane shear load, then approximately 9 elements per half wave is needed in order to get results that are below a tolerance of 5 % error, see Figure 28. This is also validated when the same plates are investigated, but this time with clamped boundary conditions. The difference between clamped and simply supported conditions is that when clamped plates are considered, the buckle mode is about one whole wave over a square plate. For the case with simply supported boundary conditions, one half wave is obtained over the plate, see Figure 25.

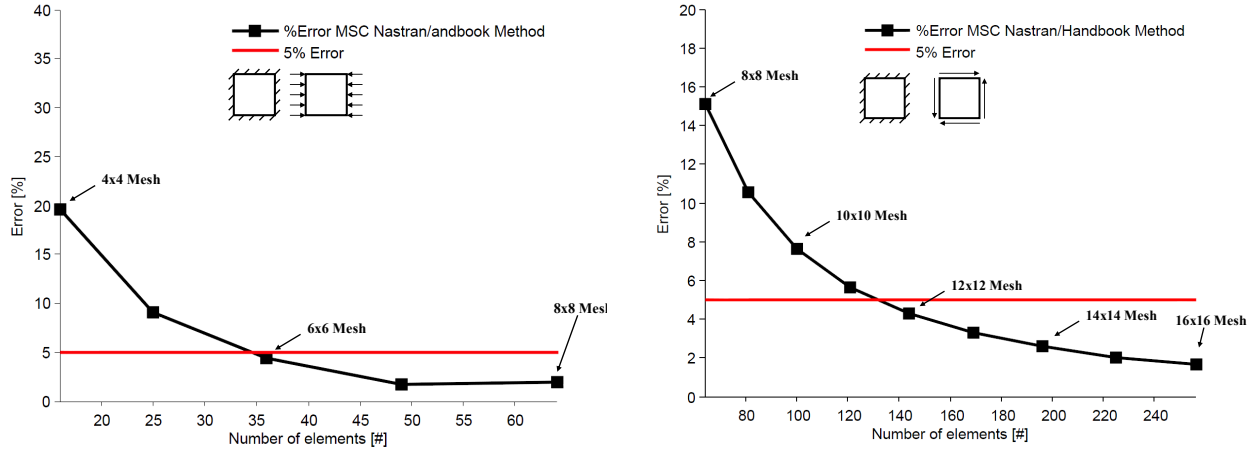


Figure 29: The error between the FE results for plates meshed with 1:1 mesh density and the Saab Strength Data handbook.

The need of higher mesh density can instantly be seen in Figure 29 where it is approximately at 6x6 element mesh (compared to 4x4 for the simply supported case) and 12x12 element mesh for in-plane shear (compared to 9x9 for the simply supported case). The same trend is seen for rectangular plates where for the uniaxially compressed plates, four buckles are obtained along the longer side. For rectangular plates subjected to in-plane shear load, three buckles are obtained along the plate. See Figure 25 for contour plots of the buckle modes for the two types of load and Figure 30 – Figure 31 for numerical results.

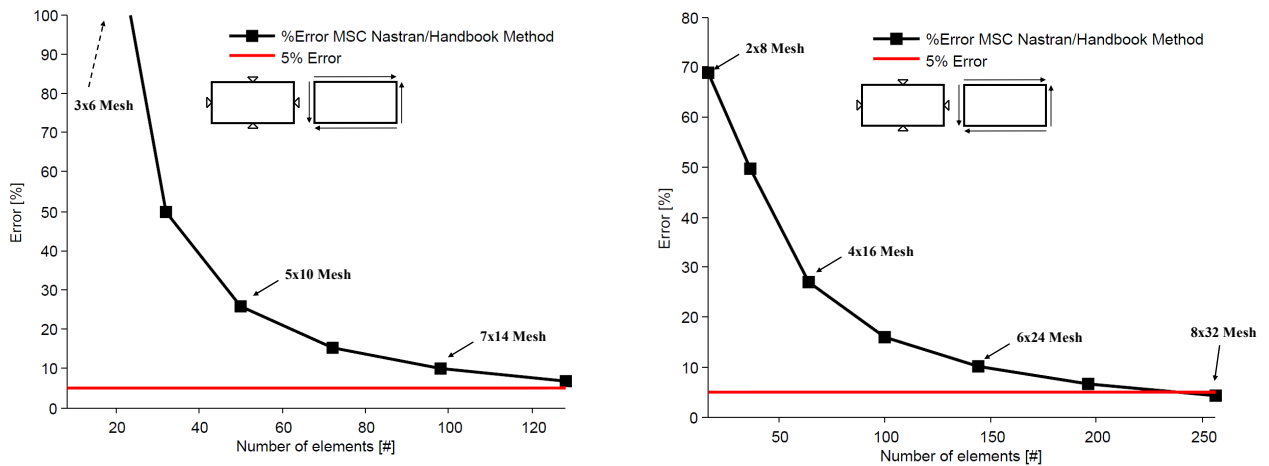


Figure 30: The error for simply supported plates loaded in in-plane shear and for various mesh densities (1:2 mesh density to the left and 1:4 mesh density to the right). The longer side of the rectangular plate is four times longer than the shorter side.

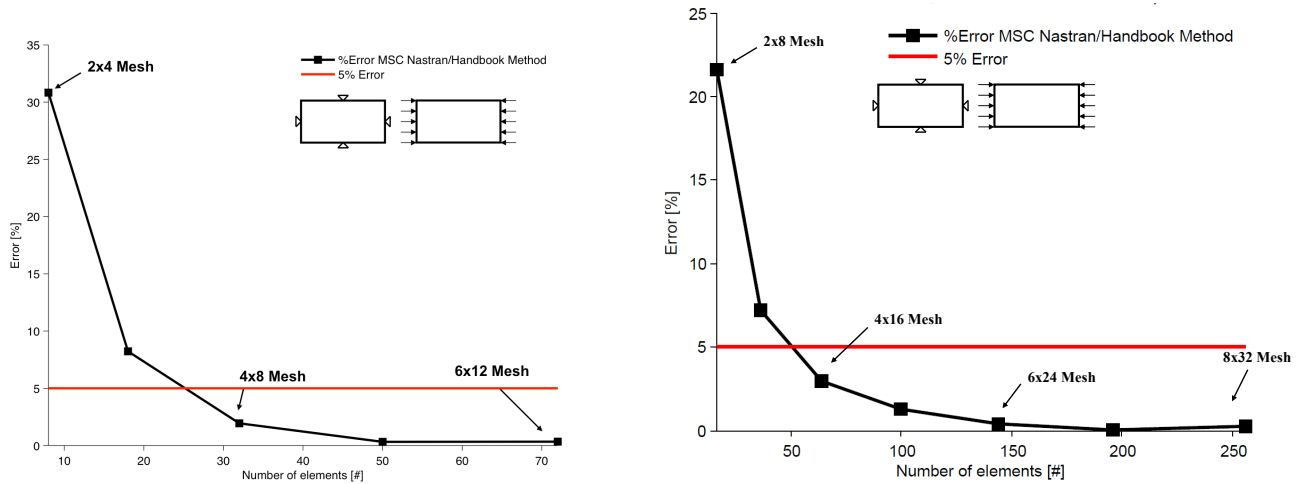


Figure 31: The error between the FE results for simply supported plated loaded in uniaxial compression for various mesh densities (1:2 to the left and 1:4 to the right) versus the Saab Strength Data handbook. The longer side of the rectangular plate is four times longer than the shorter side.

Figure 30 shows that a mesh consisting of 8x16 and 8x32 elements are needed for a simply supported rectangular plate subjected to in-plane shear load in order to be below 5 % error with respect to theory. For the case when uniaxial compression load is considered, a mesh consisting of 4x8 and 4x16 elements are sufficient, see Figure 31. Also, a study was done applying the compression force along the longer edge of the rectangular plate using 1:2 mesh density, which showed the same trend as obtained earlier.

Summarizing all the obtained results in this subpart, it can be concluded that the condition of 8 elements per half wave for in-plane shear load and 4 elements per half wave for uniaxial compression load always has to be fulfilled.

6.1.2 Part 1.2

In the second part of the parametric study, the buckling load for plates was evaluated against the current Saab Strength Data handbook. Figure 32 show that the linear buckling analysis is very accurate for slender plates (for both uniaxial compression and in-plane shear), which buckles due to geometrical instability before the yield limit of the material.

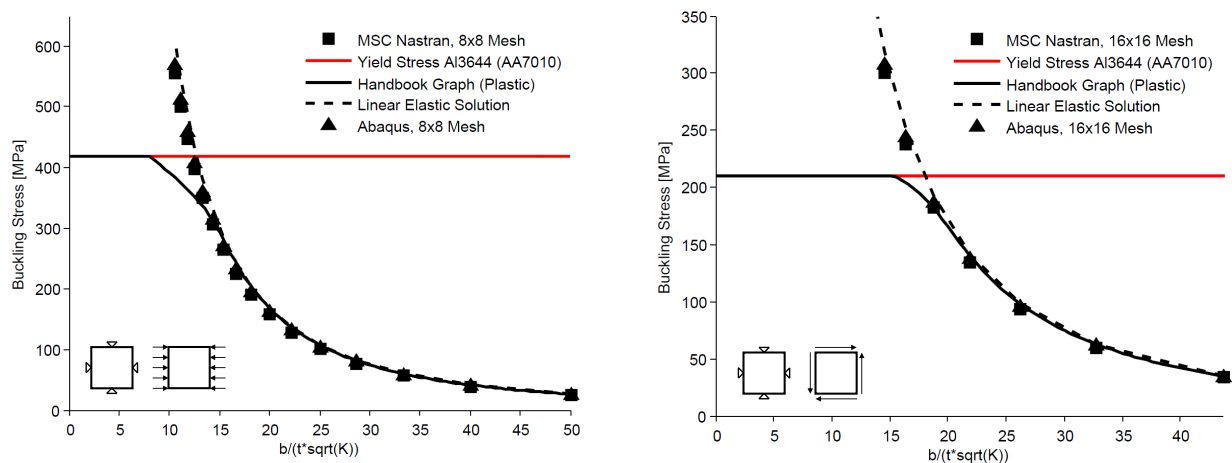


Figure 32: The results obtained from the linear buckling analyses compared to the buckling curves in the Saab Strength Data handbook for simply supported plates and two load cases: uniaxial compression (left) and in-plane shear load (right).

When stockier plates are considered, at approximately 60% of the yield stress, the FE solution and the Saab Strength Data curves starts to differ and the linear buckling analysis is no longer sufficient to catch the buckling behavior of the plate. This is mainly due to nonlinear behavior of the material (the material starts to soften). For further studies of slender and stocky plates, see Alinia et al. (2012) and for graphs showing the relative error between the numerical results and the Saab Strength Data handbook, see Figure 61 in Appendix D.

6.1.3 Part 1.3

In Figure 33, the results from the third part of the parametric studies are illustrated where simply supported plates containing holes, both centrally and with various placements, were investigated. The plates were subjected in in-plane shear load. It is possible to see that for small holes ($d/b \leq 0.225$), the result from the Strength Data handbook of Saab correlates well to the FE results. If larger holes ($d/b \geq 0.225$) are considered, it is possible to see in Figure 33 that the error starts to increase and the FE results are lower (or more conservative) if compared to the Saab Strength Data handbook results.

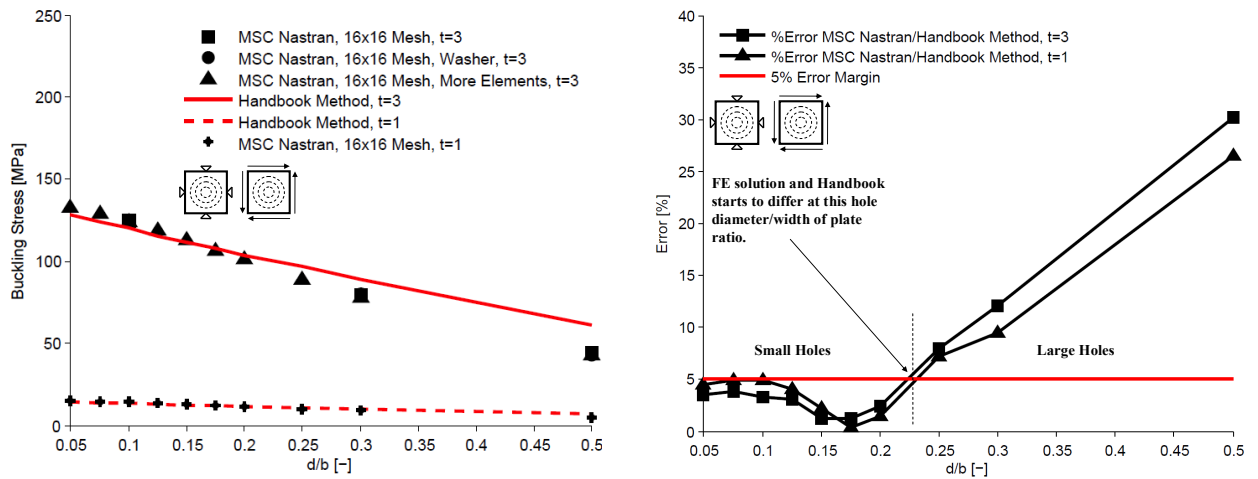


Figure 33: The results obtained from the linear buckling analyses for various diameters of a centrally placed hole (left) and for two different thicknesses. The plates are simply supported and loaded in in-plane shear load.

The reason for this is still unclear, but it may be that the buckling goes from a global buckling of the plate to a more local buckling around the hole for a larger hole diameter/width ratio of the plate (see Figure 26 for a contour plot showing the buckling mode). This may not be considered by the theory that the Saab Strength Data handbook is based on and therefore cause wrong results.

When various placements are evaluated, see Figure 34 and Table 6, it is possible to see that plates containing holes that have diameters that fulfill the condition $0.1 \leq d/b$ should be used with carefulness if the hole is placed in the compression diagonal.

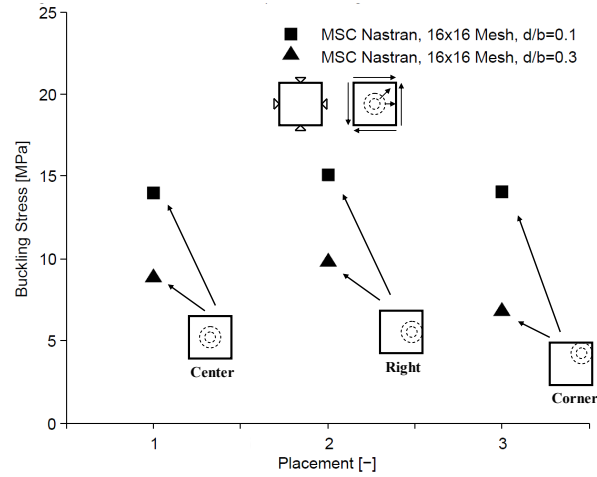


Figure 34: The results obtained from the linear buckling analyses for 20mm and 60mm diameters of a hole. Three types of eccentricities were tested and validated for a simply supported plate loaded in in-plane shear, where it is possible to see that a centrally placed hole is not the most conservative case if d/b ratio is somewhere between 0.1 and 0.3.

In this case, if the Saab Strength Data handbook for the centrally placed holes is used (which is considered as the extreme case), then the buckling resistance will be overestimated and not give conservative and safe results. For deeper studies on plates containing eccentrically placed holes under various boundary conditions and load types, see Narayan and Chow (1984).

Table 6: The results obtained regarding the variation of buckling stress with the placement (Figure 33) in numbers.

Results	σ_{cr}^{Center} [MPa]	σ_{cr}^{Right} [MPa]	σ_{cr}^{Corner} [MPa]
$d/b = 0.1$	13.98	15.09	14.05
$d/b = 0.3$	8.92	9.87	6.87

6.1.4 Part 1.4

Results from the fourth subpart is presented in Figure 35 and it can be seen that when modeling plates with steps, then a reduction of buckling resistance is obtained as the thickness ratio is increased.

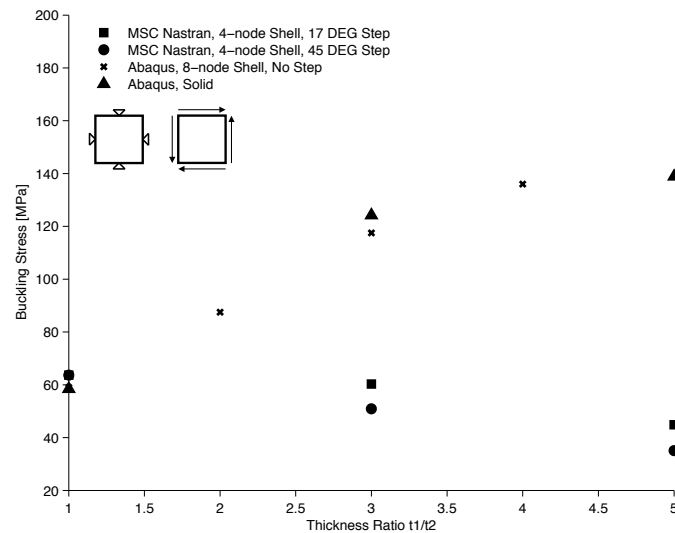


Figure 35: The results obtained from the linear buckling analyses for various step angles and thickness ratios between the plate and landing. The plates are simply supported and loaded in in-plane shear.

This is very misleading and clearly shows that the landings of reinforced plates should be modeled in the same plane as the plate itself if the structural modeling problem is going to be discretized using shell elements.

As the angle and the length of the step increases, the buckling load reduces further and the contour plot containing the first eigenmode in Figure 27 shows that for a increased thickness ratio, the buckling mode pattern moves from the landings and gets more concentrated to the middle of the plate. This makes it more look like a case where all four edges are clamped instead of simply supported.

6.1.5 Part 1.5

The nonlinear buckling analyses in fifth subpart of the parametric study with corresponding illustrations in Figure 36 and Figure 37 shows that exactly the same results are obtained in both MSC Nastran and Abaqus, for two load cases. Furthermore, the imperfection sensitivity analysis in the same picture show that a plate loaded in uniaxial compression is more sensitive to imperfections and buckles more abruptly if compared to a plate subjected to in-plane shear load.

If too large imperfection is applied to a model, then the behavior goes from a buckling problem to a deformation problem that takes place over a large force interval and the buckling resistance of a structure decreases a lot. The amount of imperfections used should be maximum five percent of thickness in order to keep the buckling behavior. It can also be discussed if it is possible to define a critical load at these cases because the structure loses stiffness for a very short interval and then starts to once again gain stiffness.

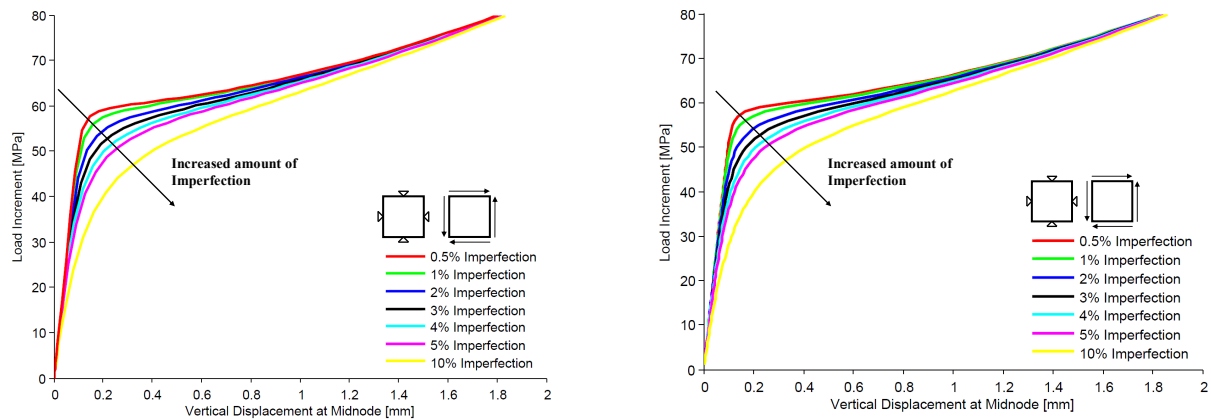


Figure 36: The impact of various amount of imperfection for MSC Nastran (left) and Abaqus (right) for a simply supported plate loaded in in-plane shear.

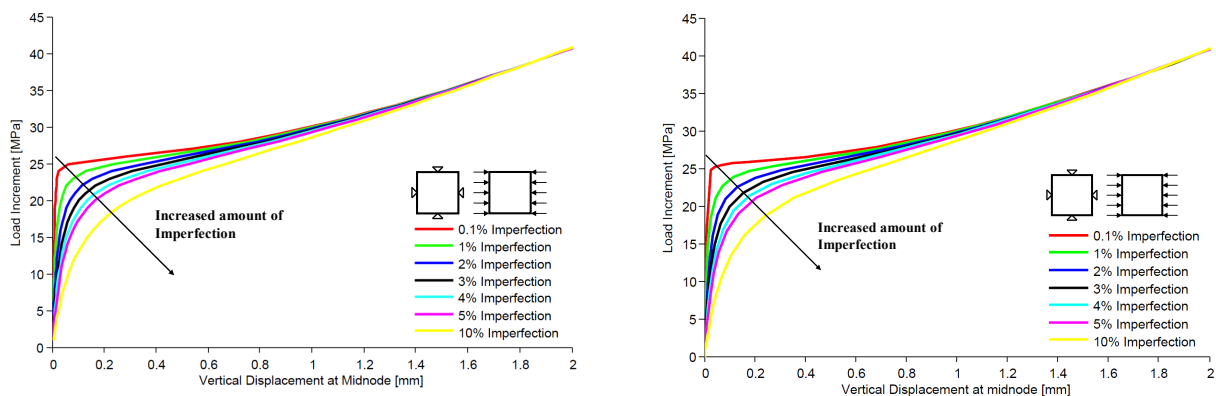


Figure 37: The impact of various amount of imperfection for MSC Nastran (left) and Abaqus (right) for a simply supported plate loaded in uniaxial compression.

The two approaches for estimating the buckling load from a buckling path is illustrated in Figure 38 and Figure 39. The differences between the obtained results when using these two methods for extracting the buckling load are presented in Figure 40 and it is possible to see that the Linearization method gives more conservative results, but this can still be quite arbitrary.

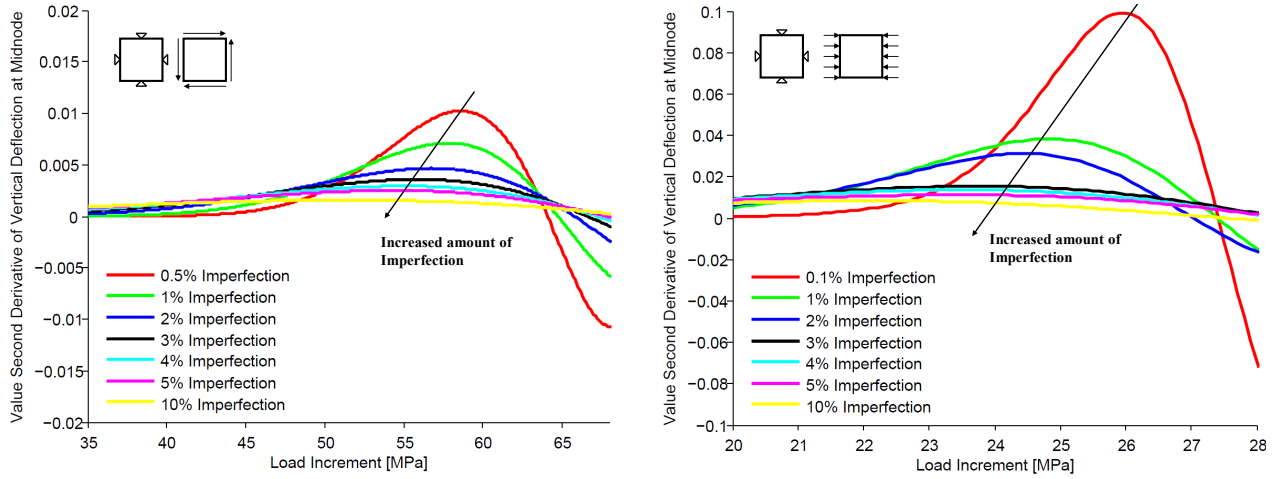


Figure 38: The Second derivative method for various amounts of imperfections. The results are from a simply supported plate loaded in in-plane shear (left) and uniaxial compression (right).

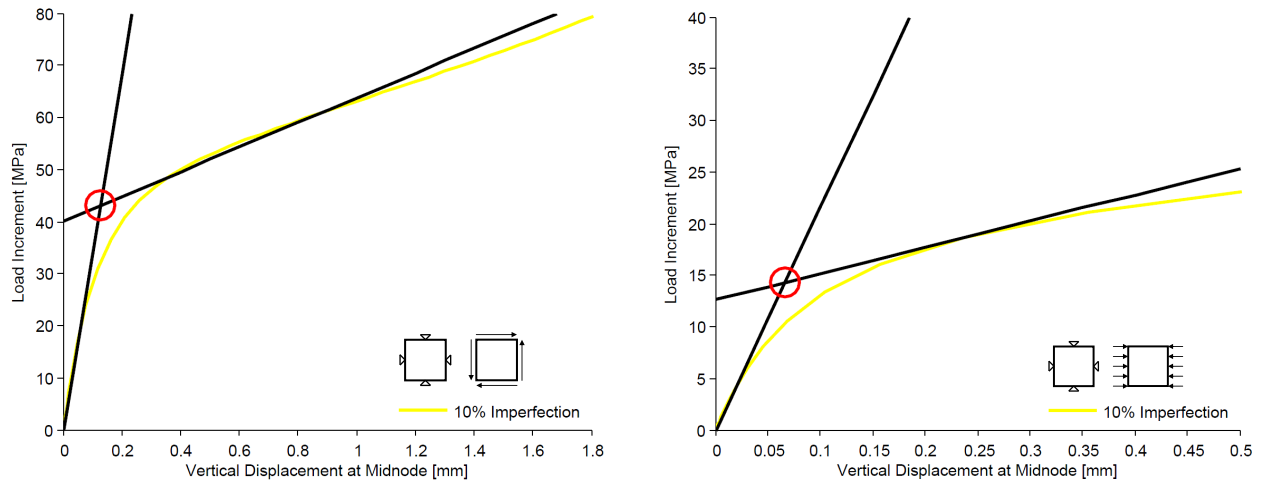


Figure 39: The Linearization method for 10% imperfection and two load cases. The results are from a simply supported plate loaded in in-plane shear (left) and uniaxial compression (right).

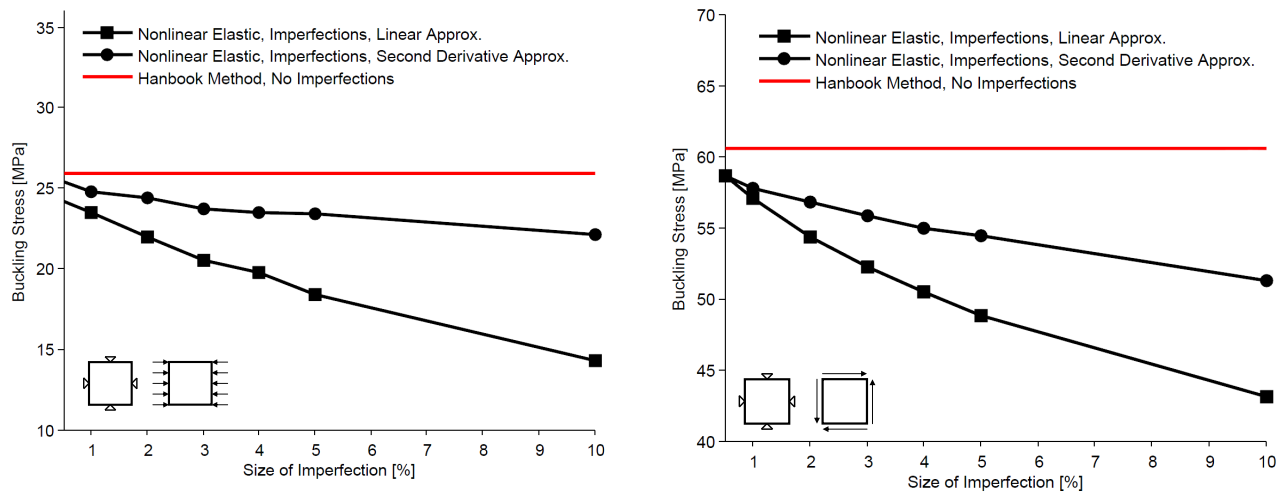


Figure 40: Summary of the results obtained in this subpart where the two approximation methods are compared to each other and the handbook method solution. It is possible to note a drop in buckling stress with the increased amount of imperfection.

The Second derivative method is more time consuming and is strongly dependent on the nonlinear solution in order to make a good curve fit. Looking at the big picture, the Linearization method is easier and much faster to use if compared to the Second derivative method and it still gives relatively good results.

6.1.6 Part 1.6

The sixth subpart of the parametric study is about using both material nonlinearity and large deformations in order to see if it is possible to catch the buckling behavior of stocky plates and compare the obtained results to the curves in the current Saab Strength Data handbook (as for Part 1.2). Stocky plates buckle closer to the yield limit of the material and the buckling are more due to material instability/bifurcation rather than geometrical instability, which was the case for slender plates.

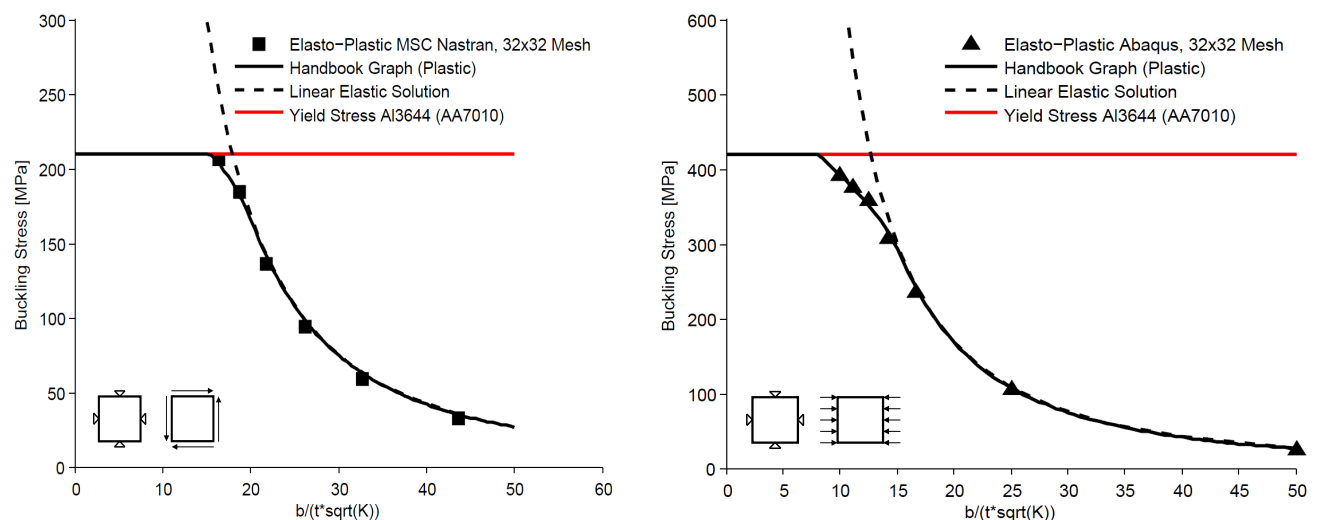


Figure 41: A comparison between the nonlinear FE results from two solvers (MSC Nastran to the left and Abaqus to the right) and the curves in the Saab Strength Data Handbook.

Figure 41 shows a good agreement between the numerical results obtained from the FE analyses and the current handbook curves, both for MSC Nastran and Abaqus. This implies that FE models are compatible with the current Saab Strength Data handbook.

6.1.7 Part 1.7 and Part 1.8

The last two parts in the parametric study (Part 1.7 and Part 1.8) are about validating Part 1.3 and Part 1.4 by using nonlinear analysis. The obtained results validate the same that was obtained in the linear buckling analyses (Figure 42 and Figure 43).

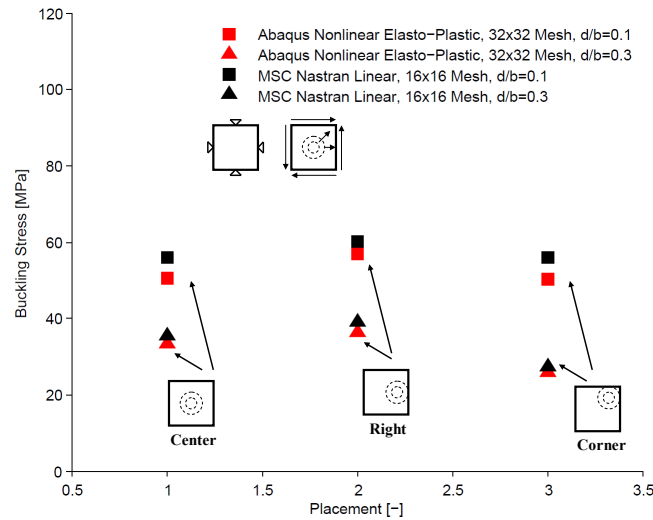


Figure 42: A comparison between the buckling stress obtained from linear and nonlinear FE models for plates with eccentric holes. It is possible to see that they follow the same pattern.

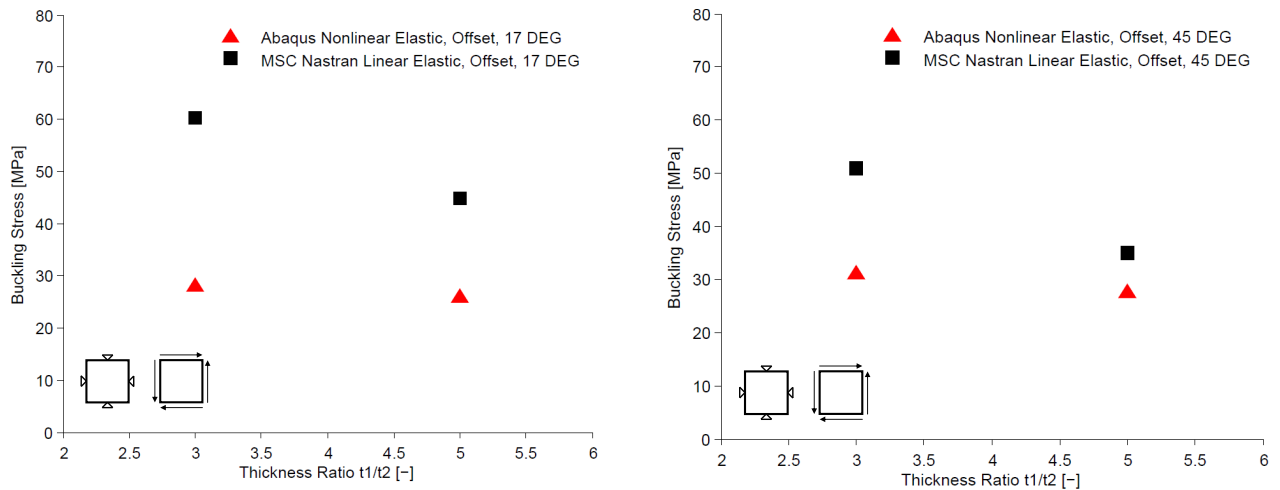


Figure 43: A comparison between the buckling stress from a linear and nonlinear FE model for plates where the landings are generated as midsurfaces for two different step angles and various thickness ratios.

6.2 Part 2

Three FE models of the test specimens were evaluated against experimentally obtained results. It is possible to see a comparison showing the buckle modes in Figure 44 – Figure 46 and the von Mises Equivalent stress distribution in Figure 62 located in Appendix E.

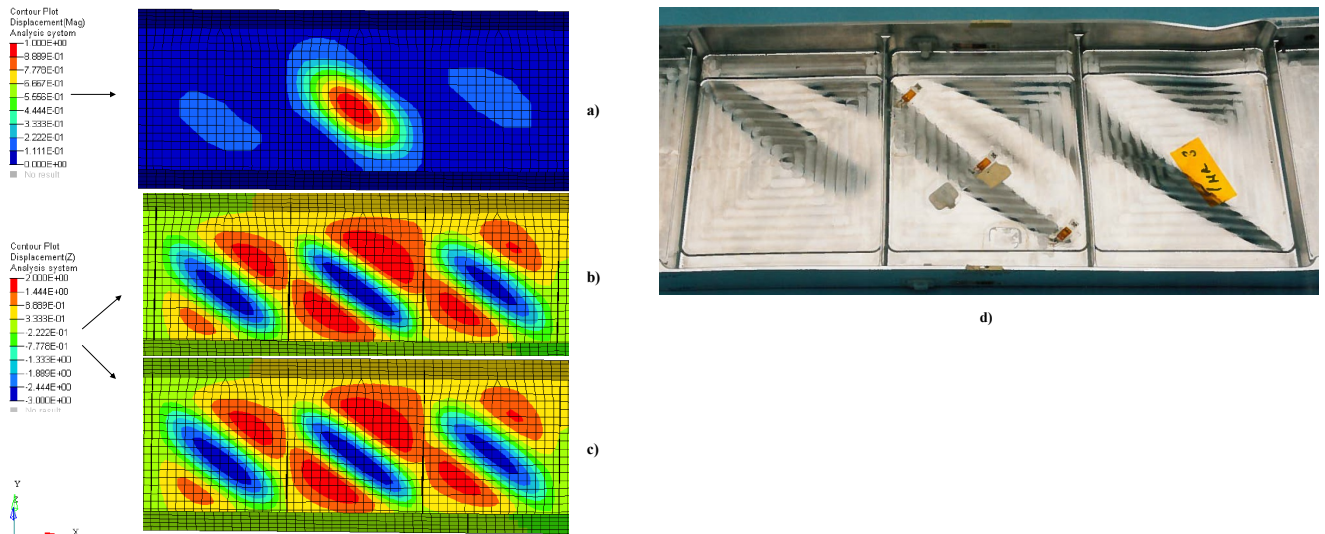


Figure 44: A comparison between the different buckling analyses and the experimentally obtained result with respect to the out-of-plane displacement for HSM Shear Web Beam Type 1 for; a) Linear buckling analysis, b) Nonlinear elastic buckling analysis at 100% load, c) Nonlinear elastic buckling analysis with 5% imperfection at 100% load and d) Experimental result for 200% load.

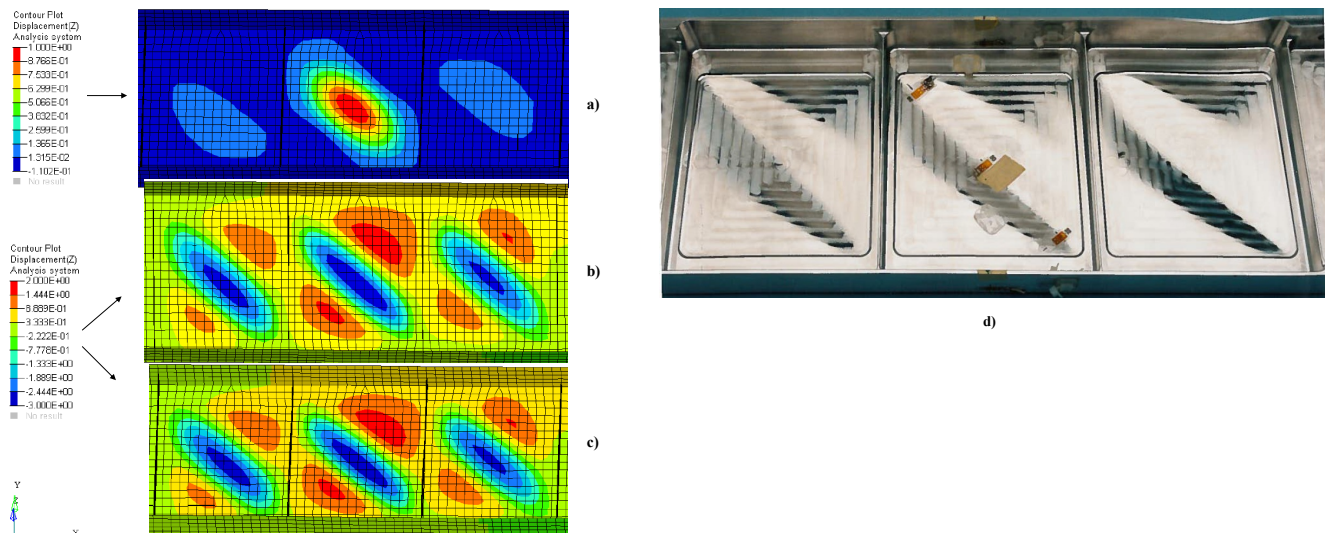


Figure 45: A comparison between the different buckling analyses and the experimentally obtained result with respect to the out-of-plane displacement for HSM Shear Web Beam Type 5 for; a) Linear buckling analysis, b) Nonlinear elastic buckling analysis at 100% load, c) Nonlinear elastic buckling analysis with 5% Imperfection at 100% load and d) Experimental result for 200% load.

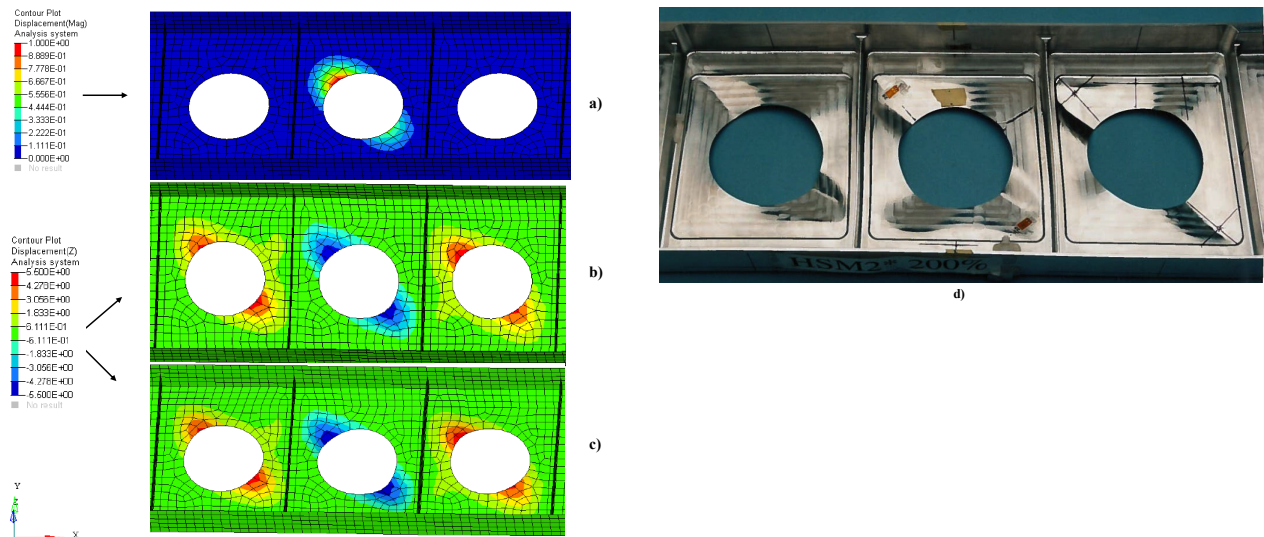


Figure 46: A comparison between the different buckling analyses and the experimentally obtained result with respect to the out-of-plane displacement for HSM Shear Web Beam Type 2 for; a) Linear buckling analysis, b) Nonlinear elastic buckling analysis at 100% load, c) Nonlinear elastic buckling analysis with 5% imperfection at 100% load and d) Experimental result for 200% load.

6.2.1 HSM Shear Web Beam Type 1

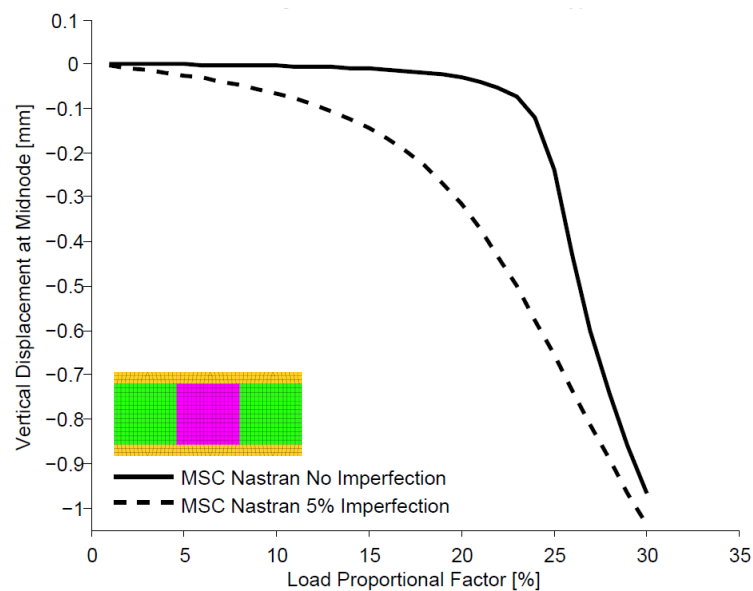


Figure 47: Postbuckling path of HSM Shear Web Beam Type 1 with and without imperfection.

6.2.2 HSM Shear Web Beam Type 5

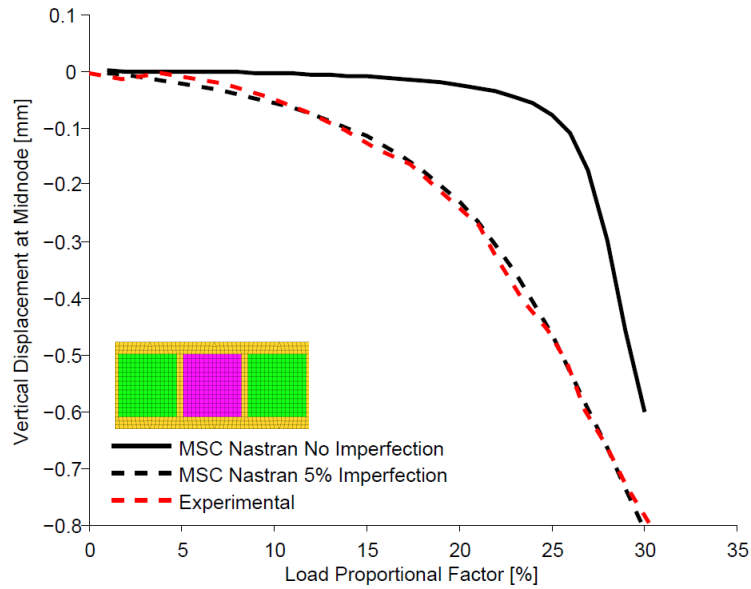


Figure 48: The postbuckling path of HSM Shear Web Beam Type 5 with and without imperfection.

6.2.3 HSM Shear Web Beam Type 2

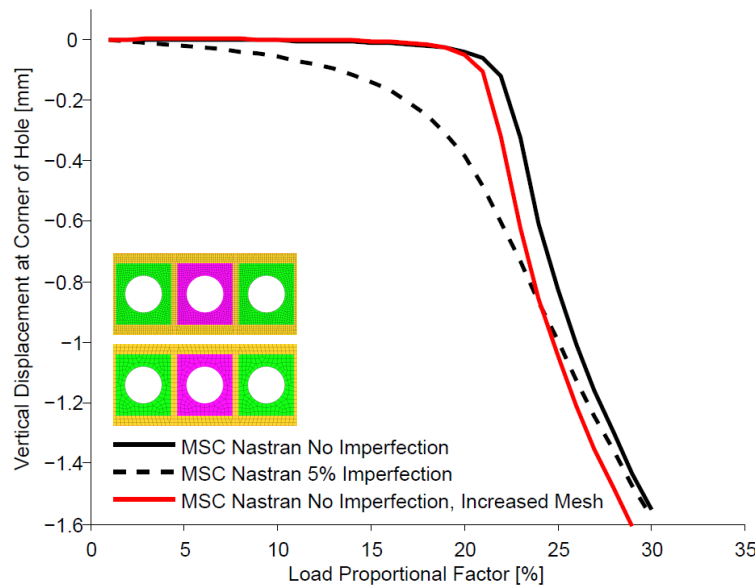


Figure 49: The postbuckling path of HSM Shear Web Beam Type 2 with and without imperfection and for two mesh densities.

6.2.4 Summary

The errors for Type 1 goes from 58% to 20% and from 17.5% to 8.33% for Type 5, see Figure 47-48 and Table 8. Type 2 does not show the same trend as the two other test specimens where the error only drops from 51.3% to 40%, see Figure 49 and Table 8. One explanation can be the large unstiffened hole ($d/b = 0.6$) that is present in this model. It was shown in the parametric studies in Part 1.3 that the results from the FE models started to differ at ratios $d/b \geq 0.225$ and give lower results if compared to handbook results. In this case, the FE models overestimated the buckling resistance of the structure, which is hard to find an explanation for. Another reason may be that the test specimen used during testing contained

more imperfections, which was not included in this analysis. Higher mesh density was introduced as a first approach to Type 2 but this did not affect the results significantly, see Figure 49.

Table 7: The obtained results for the various types of approached for estimating the buckling stress of the HSM Shear Web Beams. The result is given in percent of S, where the maximum (100%) value of S for each case was declared earlier in the FE modeling chapter. The results are for the first buckle that occurs in each HSM Shear Web beam.

Results	Linear	Nonlinear Elastic	Nonlinear Elastic, 5% Imperfection	Experimental
<i>HSM Type 1</i>	25.3%	20.0%	16.0%	16.0 %
<i>HSM Type 5</i>	28.2%	26.0%	23.0%	24.0 %
<i>HSM Type 2</i>	22.7%	21.0%	17.0%	15.0 %

Table 8: The obtained results for the various types of approaches for estimating the buckling stress of the HSM Shear Web Beams. The result is given in relative error with respect to the experimentally obtained result for each case where red color indicates a non-conservative result and green color indicates a conservative result.

Results	Linear	Nonlinear Elastic	Nonlinear Elastic, 5% Imperfection
<i>HSM Type 1</i>	58.0%	20.0%	0.00%
<i>HSM Type 5</i>	17.5%	8.33%	4.10%
<i>HSM Type 2</i>	51.3%	40.0%	13.33%

The results from the linear buckling analysis of all three specimens are presented in Table 7 and Table 8. Even though that the thickness is very small (and the stresses very low) where the buckling occurs, which indicates that buckling should occur due to geometrical instability, this approach is not sufficient for estimating the buckling load. The linear buckling analyses highly overestimates the buckling resistance of the structures where results with more than 50% higher buckling load is achieved for Type 1 and Type 2. The relative error for Type 5 is slightly lower and around 17%. The nonlinear buckling analysis of Type 1 and Type 5 shows relatively good agreement with the numerical results; see Table 7 and Table 8.

Introducing imperfections lowers the buckling resistance of the structures and therefore also the buckling load. The eigenmodes obtained in the linear buckling analyses for all three test specimens had their buckle shape in the opposite direction if compared to the tests, which leads to that the imperfection has to be applied with a negative amplitude in order to match reality. Type 2 and Type 1 shows larger imperfection sensitivity if compared to Type 5. Noticeable is that Type 2 drops from 40% to 13.33% in relative error, which is a large drop. An explanation for this may be that in Type 2 has a more local buckling pattern around the hole, which is some kind of a free edge. Applying imperfections on nodes closer to a free edge may be more crucial and have larger impact on the out-of-plane displacement measured in the same point.

In order to match the experimental results, imperfections is needed but it is once again hard to motivate the amount that has to be applied to match reality. Applying an imperfection that has a size of 5% of the thickness for Type 5, gives more or less exactly the same results as the experiments, see Figure 48.

Table 9: The obtained results using the Strength Data handbook of Saab when estimating the buckling load of the HSM Shear Web Beams.

Results	Strength Data	Experimental
<i>HSM Type 1</i>	19.7%	16.0 %
<i>HSM Type 5</i>	19.7%	24.0 %
<i>HSM Type 2</i>	13.6%	15.0 %

Table 10: The obtained results using the Strength Data handbook of Saab for estimating the buckling load of the HSM Shear Web Beams. The result is given in relative error with respect to the experimentally obtained result for each case.

Results	Strength Data
<i>HSM Type 1</i>	23.1%
<i>HSM Type 5</i>	17.9%
<i>HSM Type 2</i>	9.30%

The Saab Strength Data approach made in the beginning was a very simplified approach and the aim was to just check the experimental results, see Table 9 and Table 10. The landings were not included in this approach, which is why exactly the same results are obtained for Type 1 and Type 5.

CHAPTER 7

CONCLUSIONS & FURTHER WORK

This final chapter starts with listing the main conclusions that are drawn with respect to the obtained results and then proposals are made on further work within the area of buckling of plates using the Finite Element Method.

7.1 Conclusions

Following conclusions were made in this work:

- Minimum mesh density for a plate loaded in uniaxial compression should be at least 4 elements per half wave to get results within 5% error with respect to theory.
- Minimum mesh density for a plate loaded in in-plane shear should be at least 8 elements per half wave in order to get results within 5% error with respect to theory.
- Linear buckling analyses of in-plane shear or uniaxially compressed plates with the correct mesh density are valid for $\frac{b}{t\sqrt{K}} \geq 16$ or approximately at 60% of the yield stress for AL3644-7010 when compared to buckling curves in Strength Data handbook. In other words, it gives correct results for slender plates where buckling occurs clearly before the yield limit of the material.
- Nonlinear buckling analyses of in-plane shear or uniaxially compressed plates with correct mesh density, material nonlinearity and large displacements are fully valid with buckling curves in current Strength Data handbook of Saab.
- FE models of plates loaded in in-plane shear, containing centrally placed holes where $d/b \geq 0.225$ gives lower results with respect to the critical buckling load, when compared to current handbook method. The reason is not clear, but it might be that after a certain d/b ratio, the buckling becomes more local than global and the handbook cannot predict this. It is not clear which is most correct and further investigations will be needed.
- FE models of plates loaded in in-plane shear, containing eccentrically placed holes where the condition $0.1 \leq d/b$ is fulfilled, should be used with carefulness if placed in the compression diagonal. In this case, if the methods for the centrally placed holes are used (which is considered as the extreme case), then the buckling load will be overestimated and not give conservative results. This is also validated using nonlinear buckling analysis.
- Landings of reinforced plates should be modeled in the same plane as the plate itself if shell elements are going to be used for discretizing the problem. The landings should be represented by a change of thickness for the corresponding elements, i.e.

not with an offset or directly extracted as a midsurface from a CAD model. If this is done, then the FE model will highly underestimate the buckling resistance of the reinforced plate and give too conservative and misleading results. This result is also validated using nonlinear buckling analysis.

- Introducing imperfections are needed when performing nonlinear buckling analysis of simply supported, perfectly flat plates loaded in in-plane shear or uniaxial compression. Uniaxially compressed plates are more sensitive to imperfections if compared to plates subjected to in-plane shear load. Imperfections can significantly reduce the buckling resistance of a structure and should be used with carefulness if amplitudes over 5% of thickness are considered. Also, using too much imperfections in nonlinear buckling analysis turns the behavior into a deformation problem rather than buckling.
- Two approaches for how to estimate the critical buckling load were investigated. If speed and simplicity is of interest, then the linearization method works fine but it can give some arbitrary (and very conservative) results that show fluctuations. The second derivative approach is much more time consuming and a good buckling path is the key in order to make a good approximation.
- The nonlinear buckling results from the FE models of the Shear Web Beams shows very good agreements for Type 1 and Type 5. The FE model of HSM Shear Web Beam Type 2 containing a large hole doesn't catch the right stiffness and over predicts the buckling load of the structure.
- MSC Nastran and Abaqus are both very fast and give the same results when performing both linear and nonlinear buckling analyses. In nonlinear buckling analysis, the *IMPERFECTION keyword available in Abaqus makes it faster to scale and use the eigenmodes from the linear buckling analysis as imperfections, directly in the input file. In MSC Nastran, the imperfections must be applied using MSC Patran (pre-processor) and this extra step costs a lot of time.

7.1 Further work

The proposals for further work within this area are the following:

- Further investigations of eccentrically placed holes in simply supported plates that are loaded in uniaxial compression and in-plane shear in order to develop a methodology for these cases.
- Investigations regarding strengthening of plates containing holes using various types of stiffeners.
- Develop a methodology that can specify the amount of imperfections that need to be included when performing buckling analysis of various types of structures.

BIBLIOGRAPHY

- S. P. Timoshenko. Theory of Elastic Stability. McGraw-Hill, Inc. New York. 1936.
- M. Stein and J. Neff. Buckling Stresses of Simply Supported Rectangular Flat Plates in Shear. NACA Technical note no. 1559. 1947.
- Abaqus. Analysis User's Manual, Version 6.11, 2011. Dassault Systéms. Providence
- MSC Nastran. Analysis User's Manual, Version 2012.2, 2012. MSC Software. Newport Beach.
- HyperWorks. Desktop User's Guide, Version 12.0, 2013. Altair Engineering. Troy
- MATLAB. Documentation. Version R2012a, 2012. The MathWorks Inc. Natick
- A. K. Soh, L. C. Bian and J. Chakrabarty. Elastic/Plastic Buckling of a Composite Flat Plate subjected to Uniform edge Compression. Thin-Walled Structures. 38:247-265. 2000.
- M. M. Alinia and A. Gheitashi. Slenderness classification of Unstiffened Metal Plates under Shear Loading. Thin-Walled Structures. 48:508-518. 2010.
- M. M. Alinia, G. Soltanieh and M. Amani. Inelastic Buckling behavior of Stocky Plates under Interactive Shear and In-plane Bending. Thin-Walled Structures. 55:76-84. 2012.
- Projektarbete LiU: Bucklingsstudie – Förstyvade Paneler. LN-017497. Saab AB. Linköping. 2014
- C. A. Featherston. Imperfection Sensitivity of Flat Plates under Combined Compression and Shear. International Journal of Non-Linear Mechanics. 36:249-259. 2001.
- C. Pellegrino, E. Maiorana and C. Modena. Linear and Nonlinear behavior of Steel Plates with Circular and Rectangular Holes under Shear Loading. Thin-Walled Structures. 47:607-616. 2009.
- N. E. Shanmugam and A. Tahmasebinejad. Elastic Buckling of Uniaxially loaded skew Plates containing Openings. Thin-Walled Structures. 49:1208-1216. 2011.
- R. Narayan and F. Chow. Buckling of Plates Containing Openings. Seventh International Specialty Conference on Cold-Formed Steel Structures. St. Louis. 1984.
- W. D. Kroll. Instability in Shear of Simply Supported Square Plates with Reinforced Hole. National Bureau of Standards. Research Paper RP2037 Volume 43. 1949.
- B. Cheng and J. Zhao. Strengthening of Perforated Plates under Uniaxial Compression: Buckling Analysis. Thin-Walled Structures. 48:905-914. 2010.

- R. D. Cook, D. S. Malkus, M. E. Plesha and R. J. Witt. Concepts and Applications of Finite Element Analysis; Fourth Edition. John Wiley & Sons, Inc. 2002.
- B. Torstenfelt. Finite Elements – From the early beginning to the very end. LiU-Tryck. Linköping. 2007.
- D. O. Brush and B. O. Almroth. Buckling of Bars, Plates and Shells. McGraw-Hill, Inc. New York. 1975.
- S. P Timoshenko and S. Woinowsky-Krieger. Theory of Plates and Shells; Second Edition. McGraw-Hill, Inc. New York. 1959.
- K. Bathe. The Subspace Iteration Method – Revisited. Computers and Structures. XX:XXX-XXX. 2012
- G. Campbell, W. Ting, P. Aghssa, C. C. Hoff. Buckling and Geometric Nonlinear Analysis of a Tie Rod in MSC Nastran Version 68. Worlds Users Conference. Arlington. 1993
- S. H. Lee. Essential Considerations for Buckling Analysis. Worldwide Aerospace Conference and Technology Showcase. Toulouse. 2001
- A. Korolija. FE-Modeling of Bolted Joints in Structures. Master's Thesis. Linköping University. 2012
- M. Friberg. Evaluation report from Static Testing of HSM Shear Web Beams and Associated Testing of Similar Assembled Structure. FKH-1999-0152. Saab AB. Linköping
- Test Program for testing parts manufactured with HSM-technique. JSB3H-09-MP:604. Saab AB. Linköping. 1998
- Results from testing of HSM parts. FKH-98.119. Saab AB. Linköping. 1998
- Strength Data, SD. Saab AB's Handbook for Strength Data
- Homepage: Saabgroup. 2014. <http://www.Saabgroup.com/en/About-Saab/Company-profile/History/>

APPENDIX

Appendix A: FE model setup

5.2.1 Part 1.1

Table 11: The properties for subpart 1.1 where a mesh density study is performed for square (100mm times 100mm) and rectangular (100mm times 400mm) plates. For the case when the type of load is uniaxial compression, it is applied on the short sides of the rectangular plate.

FE Modeling

Height	100	[mm]
Width	100 and 400	[mm]
Thickness	1	[mm]
Young's Modulus	70300	[MPa]
Poisson's Ratio	0.33	
Element Type	CQUAD4/S4	-
Mesh Quantity	Varied with Ratio 1:1, 1:2, 1:4	-
Boundary Condition	Clamped/Simply Supported	-
Load Case	Uniaxial Compression/In-plane Shear	-
Load Magnitude	Unit Load	[N]
Analysis Type	Linear Buckling	-
Extraction Method	Lanczos	-
Solver	MSC Nastran/Abaqus	-

5.2.2 Part 1.2

Table 12: The properties for subpart 1.1, where the thickness is varied for the plates in order to see how well the obtained results fits the current buckling curves in the Strength Data handbook of Saab. A thicker plate gives a higher resistance to buckling and also moves the buckling point closer to the yield limit of the material.

FE Modeling

Height	100	[mm]
Width	100	[mm]
Thickness	Varied	[mm]
Young's Modulus	70300	[MPa]
Poisson's Ratio	0.33	
Element Type	CQUAD4/S4	-
Mesh Quantity	8x8	-
Boundary Condition	Simply Supported	-
Load Case	Uniaxial Compression/In-plane Shear	-
Load Magnitude	Unit Load	[N]
Analysis Type	Linear Buckling	-
Extraction Method	Lanczos	-
Solver	MSC Nastran/Abaqus	-

5.2.3 Part 1.3

Table 13: The center placement is placed at the midpoint of the plate and the placement to the right means that the hole is translated 25% of the width in the x-direction. Finally, the corner placement means that the hole is translated 25% of the width in the x-direction and y-direction. The various placements are only tested for holes with diameter 20, 40 and 60mm.

FE Modeling

Height	200	[mm]
Width	200	[mm]
Thickness	1/3	[mm]
Hole Diameter	10, 15, 20, 25, 30, 35, 40, 50, 60	[mm]
Placement	Center, Right, Corner	-
Young's Modulus	70300	[MPa]
Poisson's Ratio	0.33	-
Element Type	CQUAD4	-
Mesh Quantity	16x16	-
Boundary Condition	Simply Supported	-
Load Case	In-plane Shear Load	-
Load Magnitude	Unit Load	[N]
Analysis Type	Linear Buckling	-
Extraction Method	Lanczos	-
Solver	MSC Nastran	-

5.2.4 Part 1.4

Table 14: The properties for subpart 1.4. The thickness for the plate is held constant and the landing thickness is varied between the cases. Also the step angle is varied between 17 and 45 in order to see the effects of this parameter.

FE Modeling

Height	150	[mm]
Width	150	[mm]
Thickness Ratio	3/5	-
Thickness of Landing	4.5/7.5	[mm]
Thickness of Plate	1.5/1.5	[mm]
Step Angle	17/45	[Degrees]
Young's Modulus	70300	[MPa]
Poisson's Ratio	0.33	-
Element Type	CQUAD4	-
Mesh Quantity	12x12	-
Boundary Condition	Simply Supported	-
Load Case	In-plane Shear	-
Load Magnitude	Unit Load	[N]
Analysis Type	Linear Buckling	-
Extraction Method	Lanczos	-
Solver	MSC Nastran	-

5.2.5 Part 1.5

Table 15: The properties for subpart 1.5. The value of the compression modulus is used for the material properties in the FE model because that is what used when creating the buckling curves in the Strength Data handbook of Saab. Here the amount of imperfection is varied in order to investigate the imperfection sensitivity of two types of load.

FE Modeling

Height	100	[mm]
Width	100	[mm]
Thickness	1	[mm]
Young's Modulus	73100	[MPa]
Poisson's Ratio	0.33	-
Element Type	CQUAD/S4	-
Mesh Quantity	32x32	-
Boundary Condition	Simply Supported	-
Load Case	In-plane Shear/Uniaxial Compression	-
Load Magnitude	Incremental	[N]
Analysis Type	Nonlinear Elastic Buckling	-
Solution Algorithm	Newton-Raphson	-
Size of Imperfection	0.1, 0.5, 1, 2, 3, 4, 5, 10	[%]
Solver	MSC Nastran/Abaqus	-
Approximation Method	Linearization/Second derivative	-

5.2.6 Part 1.6

Table 16: The properties for subpart 1.6. The value of the compression modulus is used for the material properties in the FE model because that is what used when creating the buckling curves in the Strength Data handbook of Saab. The thickness is varied for the plates in order to see how well the obtained results fits the current buckling curves in the handbook.

FE Modeling

Height	100	[mm]
Width	100	[mm]
Thickness	0.75, 1, 1.25, 1.5, 1.75, 2/1, 2, 3, 3.5, 4, 4.5, 5	[mm]
Young's Modulus	73100	[MPa]
Poisson's Ratio	0.33	-
Plastic Properties	Material Curve	-
Hardening	Isotropic	-
Yield Function	Von Mises	-
Element Type	CQUAD4/S4	-
Mesh Quantity	32x32	-
Boundary Condition	Simply Supported	-
Load Case	In-plane Shear/ Uniaxial Compression	-
Load Magnitude	Incremental	[N]
Analysis Type	Nonlinear Elasto-Plastic Buckling	-
Solution Algorithm	Riks	-
Size of Imperfection	0.50/0.10	[%]
Solver	MSC Nastran/Abaqus	-
Approximation Method	Linearization	-

5.2.7 Part 1.7

Table 17: The properties for subpart 1.7.

FE Modeling

<i>Height</i>	200	[mm]
<i>Width</i>	200	[mm]
<i>Thickness</i>	1	[mm]
<i>Hole Diameter</i>	20/60	[mm]
<i>Placement</i>	Center, Right, Corner	
<i>Young's Modulus</i>	70300	[MPa]
<i>Poisson's Ratio</i>	0.33	-
<i>Plastic Properties</i>	Material Curve	-
<i>Hardening</i>	Isotropic	-
<i>Yield Function</i>	Von Mises	-
<i>Element Type</i>	S4	-
<i>Mesh Quantity</i>	32x32	-
<i>Boundary Condition</i>	Simply Supported	-
<i>Load Case</i>	In-plane Shear	-
<i>Load Magnitude</i>	Incremental	[N]
<i>Analysis Type</i>	Nonlinear Elasto-Plastic Buckling	-
<i>Solution Algorithm</i>	Riks	-
<i>Size of Imperfection</i>	0.75	[%]
<i>Solver</i>	Abaqus	-
<i>Approximation Method</i>	Linearization	-

5.2.8 Part 1.8

Table 18: The properties for subpart 1.8.

FE Modeling

<i>Height</i>	150	[mm]
<i>Width</i>	150	[mm]
<i>Thickness Ratio</i>	3/5	-
<i>Thickness of Landing</i>	4.5/7.5	[mm]
<i>Thickness of Plate</i>	1.5/1.5	[mm]
<i>Step Angle</i>	17/45	[Degrees]
<i>Young's Modulus</i>	70300	[MPa]
<i>Poisson's Ratio</i>	0.33	-
<i>Plastic Properties</i>	Material Curve	-
<i>Hardening</i>	Isotropic	-
<i>Yield Function</i>	Von Mises	-
<i>Element Type</i>	S4	-
<i>Mesh Quantity</i>	12x12	-
<i>Boundary Condition</i>	Simply Supported	-
<i>Load Case</i>	In-plane Shear	-
<i>Load Magnitude</i>	Incremental	[N]
<i>Analysis Type</i>	Nonlinear Elastic Buckling	-
<i>Solution Algorithm</i>	Riks	-
<i>Imperfection</i>	0.1	[%]
<i>Solver</i>	Abaqus	-
<i>Approximation Method</i>	Linearization	-

Appendix B: HSM Shear Web Beam Drawings

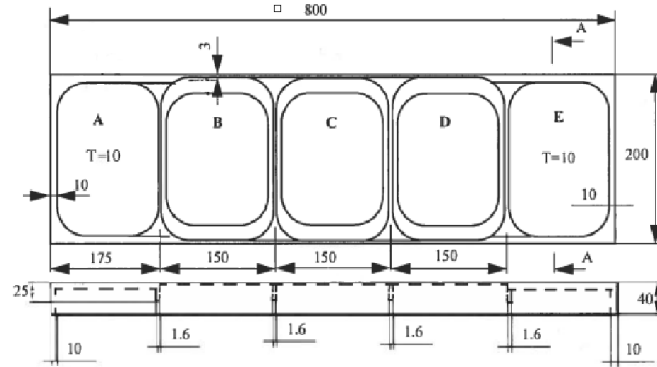


Figure 50: Drawing of the entire HSM Shear Web Beam.

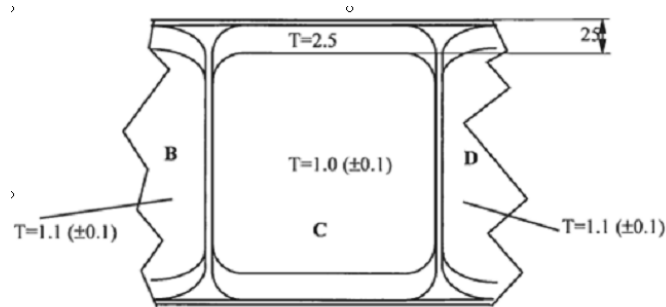


Figure 51: A close up drawing of HSM Shear Web Beam type 1

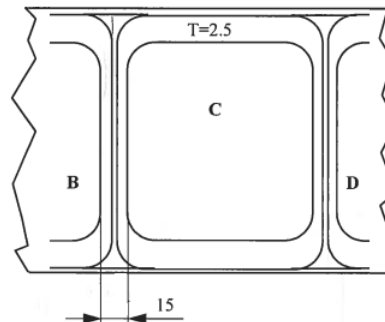


Figure 52: A close up drawing of HSM Shear Web Beam type 5.

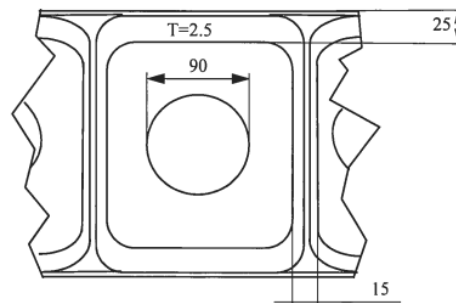


Figure 53: A close up drawing of HSM Shear Web Beam type 2.

Appendix C: Pictures from Experiments on HSM Shear Web Beam

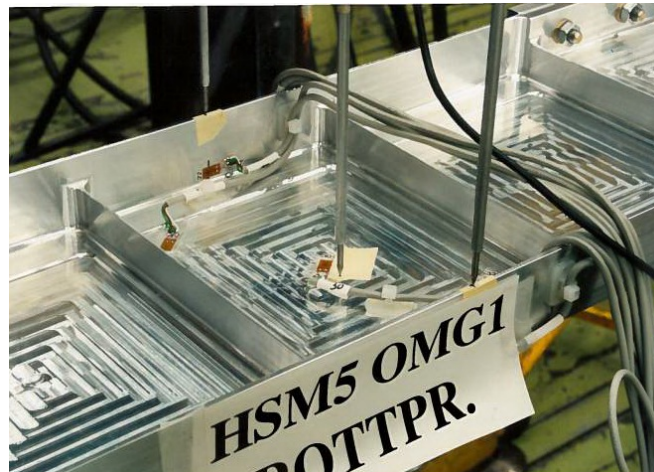


Figure 54: The displacement gauges.

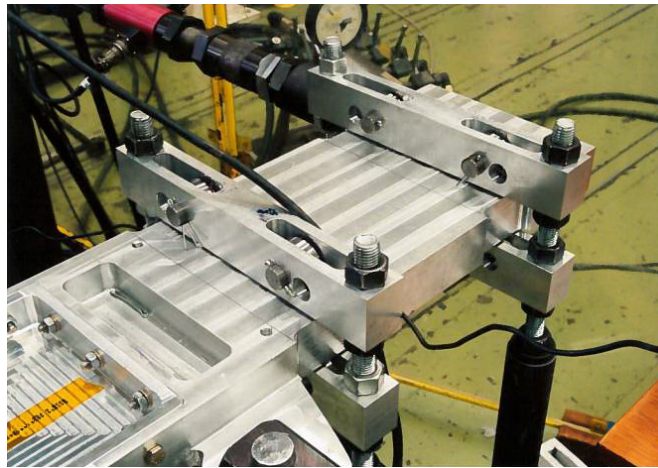


Figure 55: The cylinders, which is used for applying the in-plane force on to the Shear Web Beam.

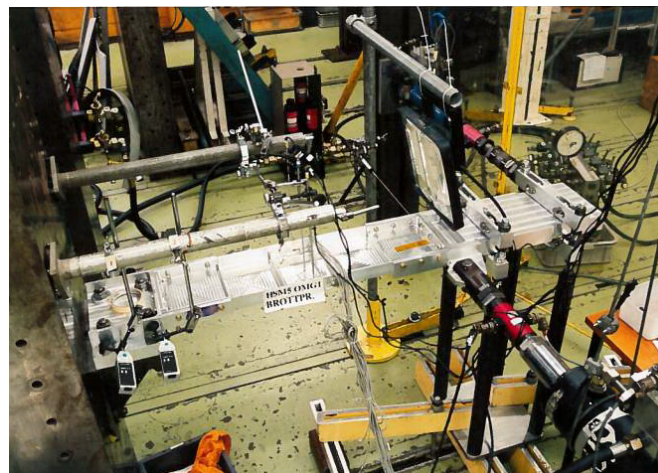


Figure 56: Overall view of the experimental setup.

Appendix D: Graphs

Part 1.1

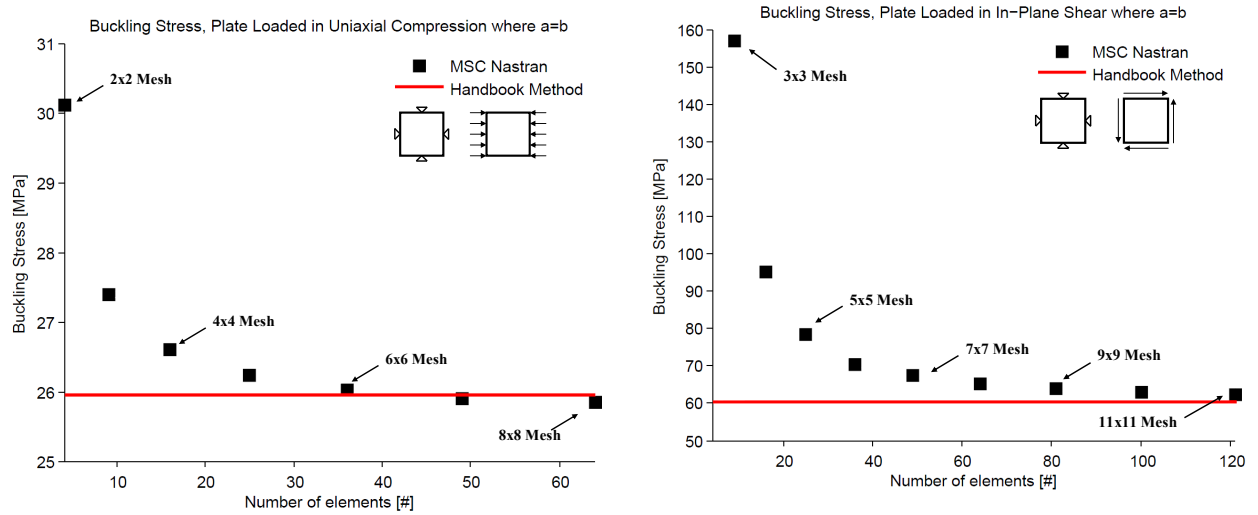


Figure 57: The buckling stress as a function of mesh density for simply supported, square plates and two load types; uniaxial compression (left) and in-plane shear load (right).

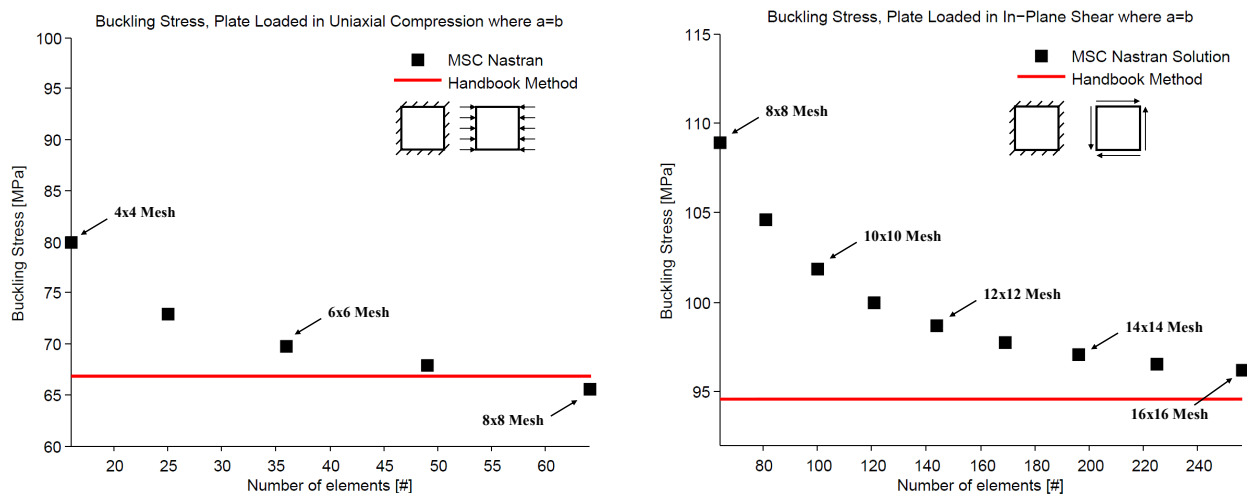


Figure 58: The buckling stress as a function of mesh density for clamped, square plates and two load types; uniaxial compression (left) and in-plane shear load (right).

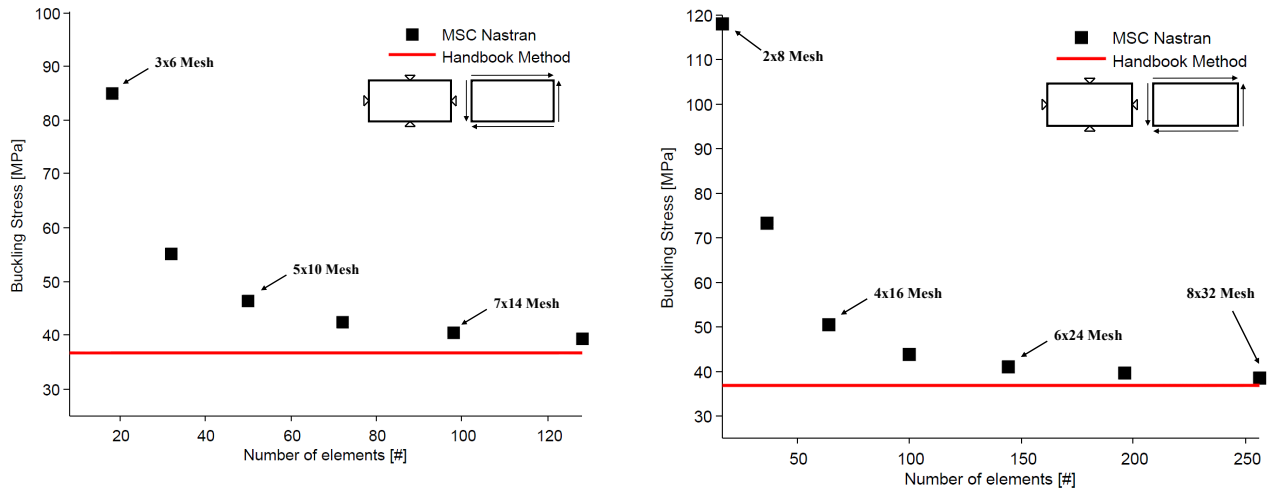


Figure 59: The buckling stress as a function of mesh density for simply supported, rectangular plates (where the longer side is four times the shorter side) subjected to in-plane shear load and two mesh ratios; 1:2 (left) and 1:4 (right).

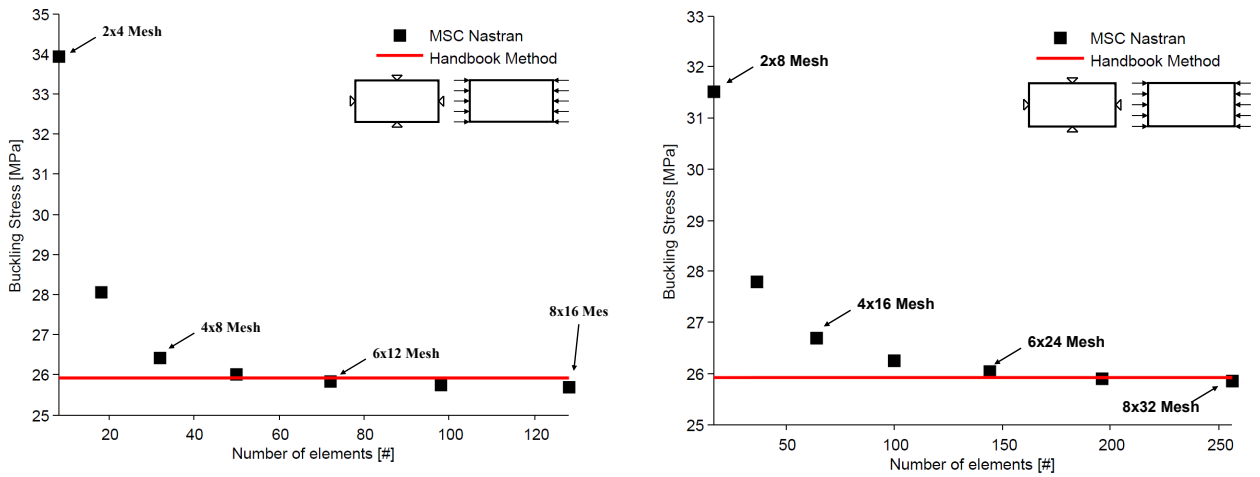


Figure 60: The buckling stress as a function of mesh density for simply supported, rectangular plates (where the longer side is four times the shorter side) subjected to uniaxial compression load and two mesh ratios; 1:2 (left) and 1:4 (right).

Part 1.2

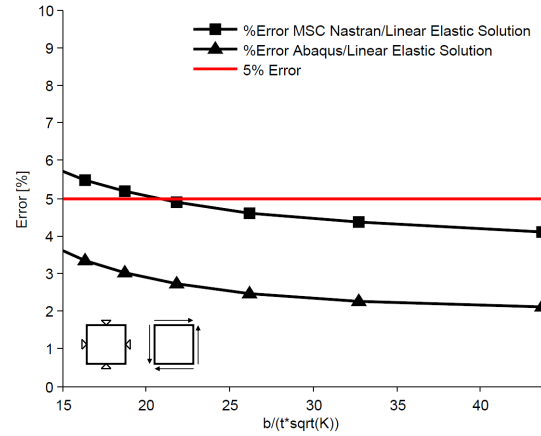
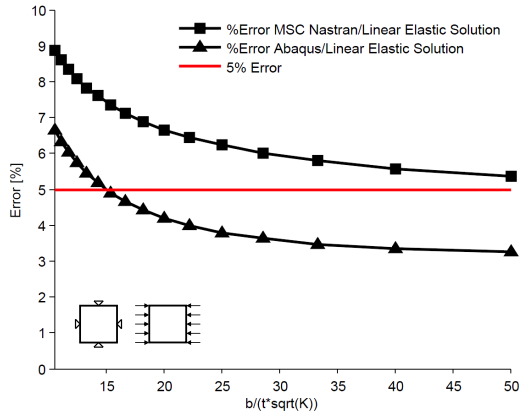


Figure 61: The error between the Saab Strength Data handbook method and FE result from MSC Nastran and Abaqus for various thicknesses and two load types (uniaxial compression to the left and in-plane shear load to the right). It is possible to see an increase of error as the thickness is increased.

Appendix E: Contour Plots

Part 2

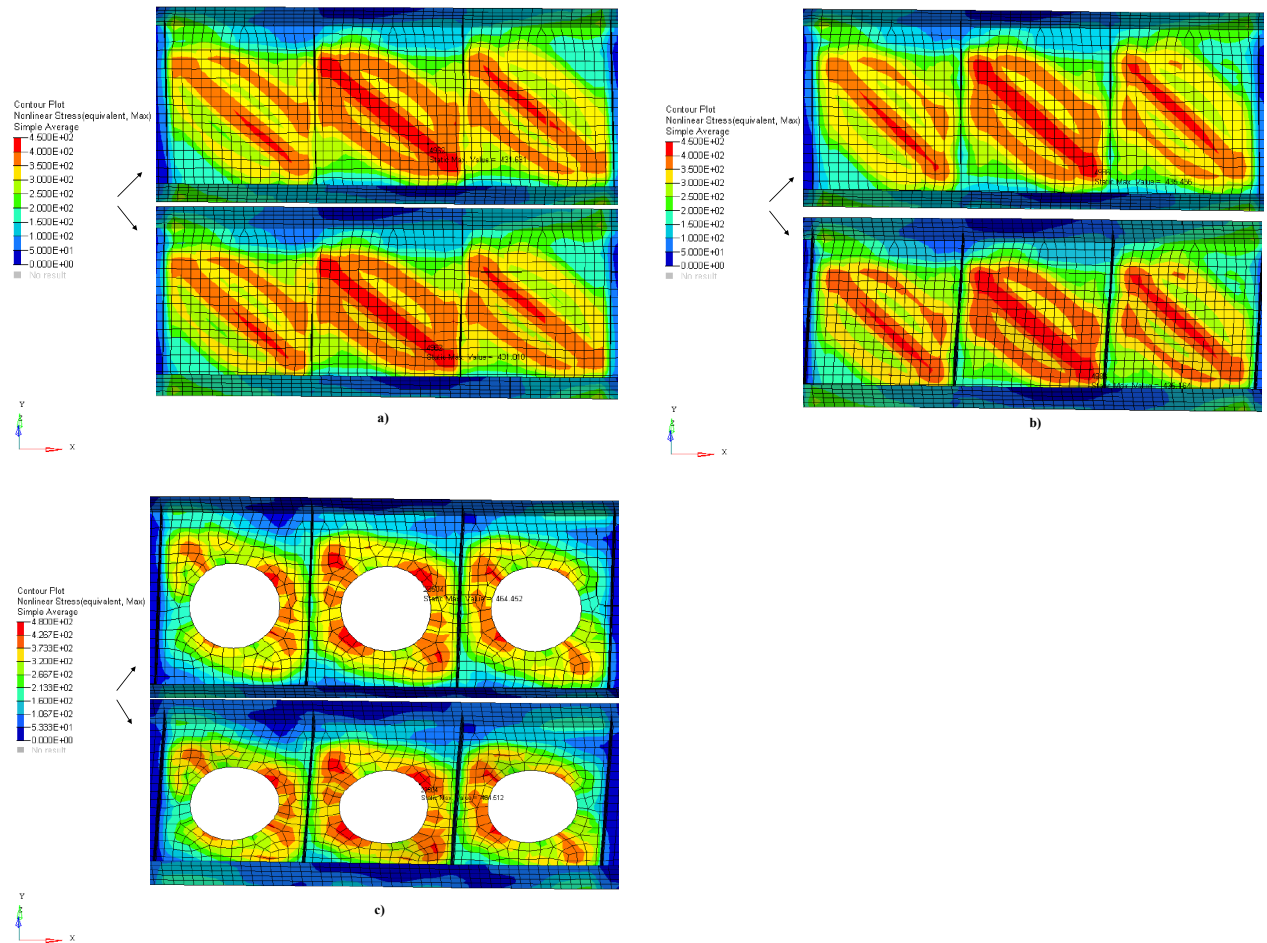


Figure 62: The von Mises equivalent stress distribution for; a) HSM Shear Web Beam Type 1, b) HSM Shear Web Beam Type 5 and c) HSM Shear Web Beam Type 2.